AFRL-AFOSR-VA-TR-2017-0001

The Oxidation and Ignition of Jet Fuels

MATTHEW Oehlschlaeger
RENSSELAER POLYTECHNIC INST TROY NY
100 8TH STREET
TROY, NY 12180

01/03/2017
Final Report

Air Force Research Laboratory
AF Office Of Scientific Research (AFOSR)/RTA1

REPORT DOCUMENTATION PAGE

Form Approved
OMB No. 0704-0188

1. REPORT DATE *(DD-MM-YYYY)*	2. REPORT TYPE	3. DATES COVERED *(From - To)*
02/12/2016	Final Technical	15-09-2011 to 14-09-2016

4. TITLE AND SUBTITLE
The Oxidation and Ignition of Jet Fuels

5a. CONTRACT NUMBER

5b. GRANT NUMBER
FA9550-11-1-0261

5c. PROGRAM ELEMENT NUMBER

6. AUTHOR(S)
Prof. Matthew A. Oehlschlaeger

5d. PROJECT NUMBER

5e. TASK NUMBER

5f. WORK UNIT NUMBER

7. PERFORMING ORGANIZATION NAME(S) AND ADDRESS(ES)
Rensselaer Polytechnic Institute
Mechanical, Aerospace, and Nuclear Engineering Department
Troy, NY 12180

8. PERFORMING ORGANIZATION REPORT NUMBER

9. SPONSORING/MONITORING AGENCY NAME(S) AND ADDRESS(ES)
Air Force Office of Scientific Research
875 North Randolph Street
Suite 325
Arlington, VA 22203-1768

10. SPONSOR/MONITOR'S ACRONYM(S)

11. SPONSOR/MONITOR'S REPORT NUMBER(S)

12. DISTRIBUTION/AVAILABILITY STATEMENT
DISTRIBUTION A: Distribution approved for public release.

13. SUPPLEMENTARY NOTES

14. ABSTRACT
A series of experimental studies designed to elucidate the oxidative reactivity and ignition properties of jet fuel and its components under homogeneous (shock tube) and multiphase spray conditions are reported. The influences of molecular composition, fuel blending, fuel/air mixture, and thermodynamic condition on oxidation and ignition are quantified and targets for kinetic model and reacting flow simulation development are provided. The most important contribution of the project is the quantification of the differences in kinetic behavior and identification of reactivity timescales across the three kinetic temperature regimes of importance in combustion processes, the low, high, and NTC temperature regions.

15. SUBJECT TERMS

16. SECURITY CLASSIFICATION OF:			17. LIMITATION OF ABSTRACT	18. NUMBER OF PAGES	19a. NAME OF RESPONSIBLE PERSON
a. REPORT	b. ABSTRACT	c. THIS PAGE			Dr. Chiping Li
Unclassified	Unclassified	Unclassified	Unclassified	30	19b. TELEPHONE NUMBER *(Include area code)* 703-696-8574

Final Report
The Oxidation and Ignition of Jet Fuels

Prepared under:
Grant #: FA9550-11-1-0261

Final report submitted by:
Prof. Matthew Oehlschlaeger (P.I.)
Rensselaer Polytechnic Institute
Mechanical, Aerospace, and Nuclear Engineering Department
110 8th Street
Troy, NY 12180
oehlsm@rpi.edu

Submitted to:
Dr. Chiping Li
Air Force Office of Scientific Research
875 N. Randolph St, Ste. 325
Arlington, VA 22203
chiping.li@us.af.mil

For the period:
15 September 2011 – 14 September 2016

Contents

1. Introduction

The design and optimization of high-performance combustion-based aero-propulsion engines in part relies on the ability to quantitatively predict combustion phenomena using computational simulations. One aspect of importance in these simulations is the description of fuel oxidation resulting in the formation of major products, heat release, and undesirable gaseous and particulate pollutant emissions. Because combustion simulation involves accurate modeling of coupled chemical and transport processes, chemical kinetic models must be assessed and validated with data from controlled experiments where transport processes are not significantly important. Combustion experiments are also needed in systems where a variety of transport, phase change, and chemical kinetic effects are relevant and compete in order to understand the relative importance of these physicochemical phenomena in realistic combustion environments as well as provide validation targets for reacting flow simulations.

Experiments utilizing shock tubes, flow reactors, rapid compression machines, and jet-stirred reactors have historically been performed to develop and validate fuel oxidation kinetic models. Shock tubes have several advantages over the alternatives. They provide a near-instantaneous rise in temperature and pressure and nearly-homogeneous conditions with negligible influence from transport processes; such an environment is ideal for studying combustion chemistry at temperatures in excess of ~600 K. The one feature of the shock tube is that reaction test times are typically limited to 1-10 milliseconds behind the reflected shock wave; however, 1-10 ms is in the range of the typical residence times for gas turbine combustors or combustion time scales in internal combustion engines.

In this project a shock tube has been used to study the oxidation and autoignition of both traditional and alternative fuels and components. Many of the literature shock tube studies have focused on quantifying the ignition delay, an important kinetic parameter indicating the reactivity of a fuel/oxidizer mixture at a given condition. Ignition times provide insight into the fuel oxidation process and are widely used for developing and validating kinetic models. Many prior shock tube ignition studies have focused on smaller hydrocarbons (C1-C8), with sufficient vapor pressure at room temperature for gas-phase reactant mixture preparation. Additionally, many of the previous measurements have been made at pressures near 1 atm, using dilute mixtures (fuel concentrations of a fraction of one percent), and with argon as the bath gas (monatomic argon has advantages due to the lack of a vibrational mode). These conditions are dissimilar to those found in gas turbine jet engines or internal combustion engines, where air is the oxidizer, the fuel concentration is typically near or greater than one molar-percent, and the pressure is elevated. In recent years, several groups have begun to address the oxidation and ignition of larger hydrocarbons at elevated pressures using heated shock tube [1-2] and aerosol shock tube [3] techniques. Our group has developed a heated shock tube facility [2] to investigate heavier hydrocarbons. The shock tube has been employed to study the autoignition of many individual hydrocarbon compounds found in or representative of those found in jet fuels and for studies of specific jet fuels. Despite these recent efforts, there are still substantial gaps in the experimental kinetics database for larger hydrocarbon components, real transportation fuels, model fuel mixtures, and important intermediate species. There are also large ranges of conditions important in gas turbine and diesel engine operation that have gone largely unexplored. For example, there have been very few studies at diesel engine conditions (50-100 atm); the U.S. DoD uses JP-8 in diesel applications. The research efforts summarized here bridges some of these gaps and others in the kinetic literature for real fuels and components, with a focus on Air Force relevant fuels.

Ignition delay times are a critical kinetic measurement because they provide information about the overall reactivity of a fuel/oxidizer mixture but ignition delay times do not provide information about the temporal evolution of the oxidation process and transient intermediate species population during oxidation. Species time-histories, on the other hand, can indicate the extent of reaction at all

reaction times and, therefore, are very useful for the development of kinetic oxidation models. Carbon monoxide is one important species that is a direct indicator of the extent of reaction or heat release rate and is sensitive to chemistry that controls both strong ignition and NTC or two-stage ignition behavior that is observed. In the present, time resolved CO laser absorption measurements have been developed as a new kinetic target to probe both low- and high-temperature fuel oxidation.

We also have extended our research focus from gas-phase reactivity to multiphase spray ignition and combustion where, in the system considered, fuel reactivity still controls the time scales for heat release but where spray processes, evaporation, and mixing also play a role. These experiments are important for understanding relative reactivity of fuels under realistic engine conditions and for providing modeling targets for multiphase ignition simulations.

2. Experimental Methods

2.1. Shock tube

The Rensselaer heated shock tube facility (Fig. 2.1) has been described in the literature [4, J22]. In the present studies it has be used in the reflected shock mode to measure ignition delay times and CO time histories during fuel oxidation. The shock tube and mixing vessel can be heated up to 200 ˚C to allow gas-phase study of high molecular weight fuel components or multi-component fuels. Fuel/oxidizer samples can be extracted prior to experiments for chromatography/mass spectrometry inspection to ensure that the reactants have not partially decomposed due to shock tube heating or condensed on the walls [5]. Post-incident and post-reflected shock conditions are determined using the normal shock equations with incident shock velocity, measured via a series of pressure transducers, and reactant mixture thermodynamic properties as inputs. The uncertainties in the initial reflected shock temperature vary from ±1% to ±1.5% and the initial reflected shock pressure from ±1% to ±2%.

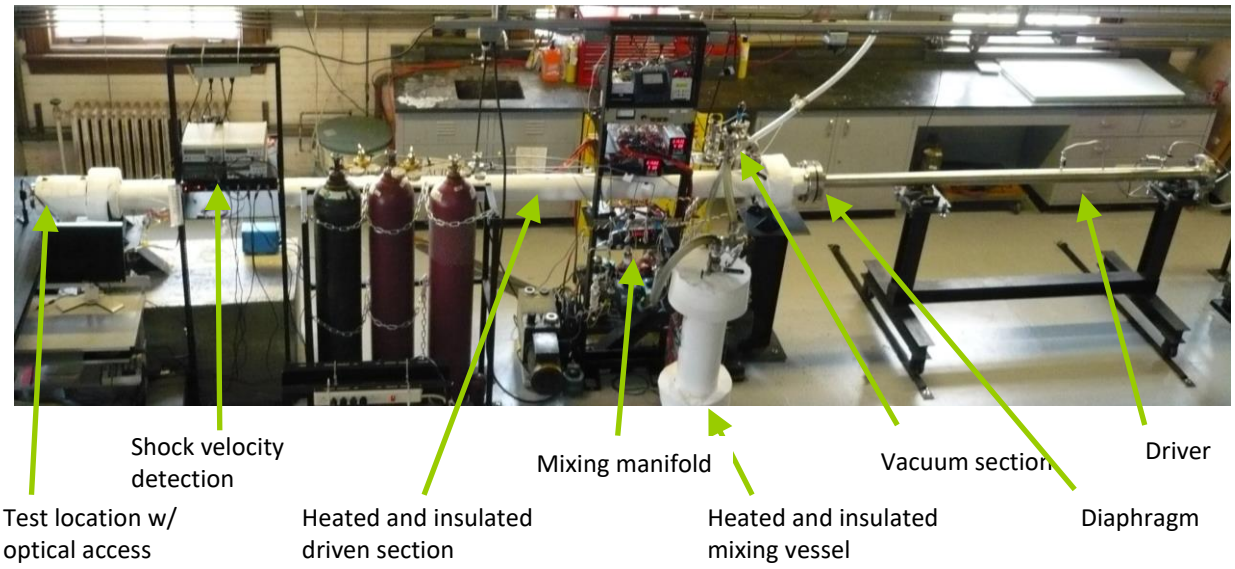

Fig. 2.1. Photograph of the RPI heated high-pressure shock tube.

For the determination of ignition delay times behind reflected shock waves, pressure and electronically-excited OH chemiluminescence are measured. See Fig. 2.2 for an example ignition delay time measurement. Ignition delay time is defined as the time interval between shock reflection at the driven section end wall, defined using a measured pressure profile at a side wall location (2 cm from end wall) and the measured incident shock velocity, and the onset of ignition at the end wall, defined by extrapolating the maximum slope in the OH signal to the baseline (acquired through the

shock tube end wall). The pressure gradient behind the reflected shock wave, due to viscous gasdynamics, for these experiments is typically in the range of 2-3% of the initial pressure per millisecond. This pressure gradient is considered in kinetic modeling of ignition delay times longer than 1-2 ms where it affects model predictions. Ignition delay times have estimated uncertainties that vary from ±15% to ±25% based on uncertainties in determination of ignition delay time from measured signals and the uncertainties in reactant mixture composition and reflected shock conditions. The uncertainty in reflected shock temperature (±1-1.5%), based on uncertainty in incident shock velocity, has the largest contribution to ignition delay time uncertainty.

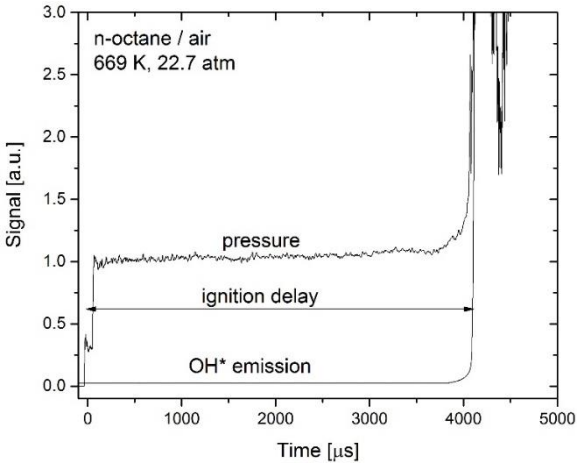

Fig. 2.2. Example ignition delay time measurement: pressure and OH* signals.

2.2. Mid-infrared CO absorption

Methods have been developed for the time-resolved measurement of carbon monoxide (CO) during the oxidation of dilute fuel/O_2/Ar mixtures at pressures up to 10 atm, following reflected shock heating, at intermediate- to low-temperature combustion conditions. CO is monitored using fixed-frequency mid-infrared line-of-sight laser absorption in the strong fundamental rovibrational band at 4.6 μm. Our approach to CO laser absorption measurements has been described previously in studies where scanned-wavelength [6] and wavelength-modulation spectroscopy [7] approaches were implemented. In the present program, a simpler fixed-frequency technique is applied with the same hardware previously used; see Tekawade et al. for a complete description of the method [J5]. CO time histories were measured using the R(9) CO transition at 2179.7719 cm^{-1}. This transition is well characterized in the literature [8-10] and isolated from interfering absorption of combustion gases at combustion conditions (see Fig. 2.3). Scanned-wavelength experiments were performed to verify predicted CO spectral absorption at the elevated pressure and temperatures considered here in the oxidation experiments. Example comparisons of scanned-wavelength measurements with spectral simulations are given in Fig. 2.4. The experiment-simulation agreement is quite good (within ±3% for absorbance at the R(9) peak).

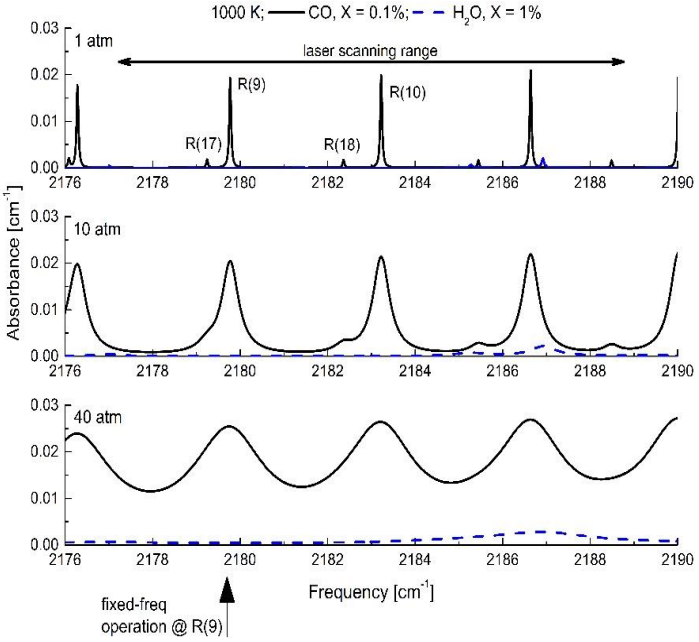

Fig. 2.3. Simulated CO and H_2O absorbance around frequency of laser operation. Simulation carried out for a mixture of 0.1% CO and 1% H_2O in argon.

For the measurement of CO during oxidation experiments, the laser was operated in fixed-frequency mode at the R(9) transition peak and CO mole fraction was extracted using Beer's law.

Signals from an example experiment are provided in Fig. 2.5, where the top panel illustrates the reference and absorption laser intensity signals and the bottom panel the pressure. Following time zero, the formation of CO causes the signal detector to reduce in intensity. At the conclusion of the shock tube test time, around 5 ms in the Fig. 2.5 example, due to the arrival of rarefaction waves from the driver, the signal detector intensity recovers slightly due to the decreased density of the test gases as indicated by the measured pressure (middle panel). The reported laser absorption measurement of CO mole fraction (examples found in Figs. 3.9 and 3.10) at known temperature and pressure is estimated at ±5% or 10 ppm, whichever is greater, based on contributions from uncertainties in the spectroscopic parameters and the system signal-to-noise.

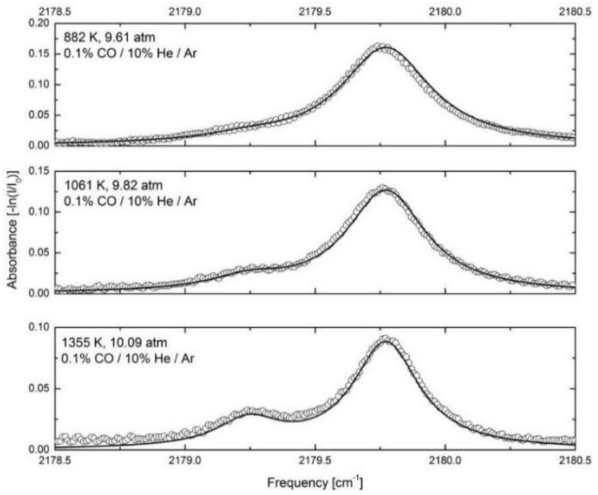

Fig. 2.4. Measured and simulated CO spectra for the R(9) and R(17) line pair for mixture of 0.1% CO, 10% He, in Ar around 10 atm and for temperatures from 882 to 1355 K.

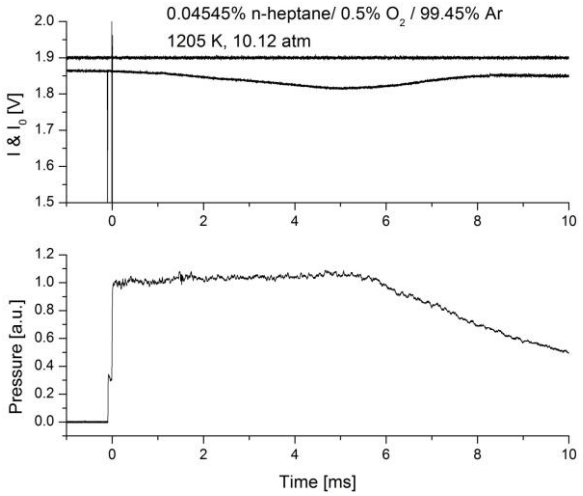

Fig. 2.5. Example measured signals for an n-heptane oxidation experiment. Top panel: both absorption signal and reference signal; bottom panel: pressure.

2.3. Constant volume spray combustion chamber

A constant volume spray combustion chamber (CVSCC) has been developed for the study of spray ignition and combustion across the low-temperature regime, at elevated pressures, and for a large range of fuel reactivity characteristic of jet fuels and their components. The CVSCC can provide derived cetane number (DCN) determinations, similar to the Ignition Quality Tester (IQT) [11]. The CVSCC is described in detail in Tekawade and Oehlschlaeger [J6]. It is a 500 mL volume electrically-heated cylindrical chamber that can operate at ambient temperatures up to 850 K and 5 MPa. Both wall and internal temperature profiles are monitored using thermocouples. A fuel injector is mounted in the top wall of the chamber to provide injection into quiescent oxidizers (typically air). Chamber and fuel line pressure are measured for ignition delay determinations.

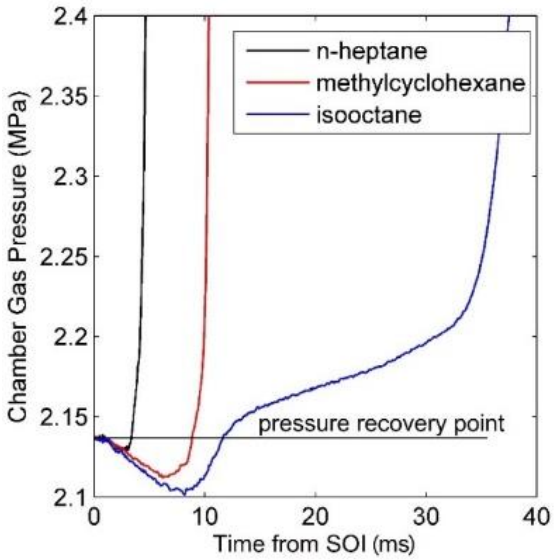

Fig. 2.6. Chamber pressure for the ignition of n-heptane, methyl cyclohexane, and iso-octane for injection into air at 818 K and 2.14 MPa.

The injector is a mechanical pintle-style diesel injector manufactured by Bosch (model W0133-1827210) that provides lower pressure injection typical of gasoline direct injection systems and much lower than modern common-rail diesel engine injection systems. The system allows the use of small fuel samples, as little as 50 mL. Additionally, the longer ignition delay times observed in the CVSCC (2-300 ms) are predominately chemistry limited, with physical effects, dependent on injection pressure, less of a controlling factor. The injection system has been characterized via high-speed imaging studies and provides an injection duration of between 4 and 15 ms with corresponding injected fuel mass of 20 to 80 mg, depending on chamber ambient pressure.

Spray ignition delay is the time interval between the start of injection (SOI) and the start of combustion (SOC). Due to the starkly different spray combustion behavior of different fuels, the definition of SOC is very important. Figure 2.6 illustrates distinct pressure behavior for three hydrocarbon compounds (n-heptane, iso-octane or 2,2,4-trimethylpentane, and methylcyclohexane) in terms of the time-history of heat release and time scale for ignition. The pre-ignition charge conditions considered in Fig. 2.6 are 2.14 MPa and 818 K and define the thermodynamic state chosen for evaluation of the DCN in IQT experiments [11]. As expected, n-heptane is the most reactive and iso-octane is the least reactive. Additionally, iso-octane shows distinct two-stage ignition behavior which complicates definition of SOC and ignition delay.

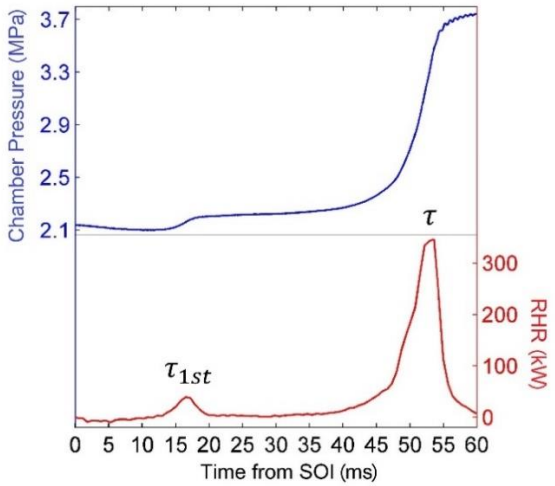

Fig. 2.7. Chamber pressure time-history and heat release rate for iso-octane injection (10.7 ms duration) into air at 767 K and 2.14 MPa.

Common definitions for SOC in spray ignition experiments are the pressure recovery point, the point at which the pressure recovers to the initial pressure, or the time at which the pressure exceeds a threshold pressure often greater than the pressure recovery point. As shown in Fig. 2.6, defining SOC using the pressure recovery point or any threshold pressure greater than the recovery point provides a similar measure of ignition delay for n-heptane or methylcyclohexane, where ignition occurs rapidly. In the case of iso-octane, a clear two-stage ignition phenomenon occurs and the definition of ignition delay is less clear. Here, we use the rate of heat release (RHR) to define ignition delay. For cases with distinct two-stage heat release we can define two ignition delays: a first-stage ignition delay τ_{1st} for the time interval between SOI and a first peak in RHR and a total ignition delay τ for the time interval between SOI and the second peak in RHR. For cases where a single-stage heat release event is observed, only a total ignition delay τ is reported as the interval between SOI and the peak in RHR. Example pressure and RHR profiles and definitions for τ_{1st} and τ are shown in Fig. 2.7 for iso-octane.

It was found in the present work that ignition delay times measured in the CVSCC correlate well with those measured in the IQT [12], allowing development of a correlation for estimation of a DCN from CVSCC ignition delay measurements made at an initial ambient condition of 818 K and 2.14 MPa, also used for measuring DCN in the IQT. A correlation was developed by fitting CVSCC ignition delay times, measured at the standard condition and using the RHR method defined above, against well-established DCNs for n-heptane (DCN=53.8), n-decane (DCN=67.2), n-dodecane (DCN=74.0), 2,6,10-trimethyldodecane (DCN=59.1), and methylcyclohexane (DCN=23.5). The correlation was fit in the same form used to define DCN in the IQT, a linear function between DCN and inverse ignition delay measured at the standard condition (τ): $DCN = \frac{216.1}{\tau} + 3.4$, where the correlation was determined by linear least-squares and yields an R^2 value of 0.9989. As seen in Fig. 2.8, the correlation provides good prediction of DCN from 25 to 75, a similar range of DCN as that for which the equation 2 form is valid in IQT experiments, and covers the range of reactivity for most of the fuels and blends considered in the present study. The repeatability of spray ignition delay measurements in the present study was the greater of either ±3% or ±0.1 ms, resulting in a repeatability for DCN determinations of ±2.5 for a DCN of 75, ±2.0 for a DCN of 70, ±1.5 for a DCN of 53, and ±1.0 for a DCN of 36 to 25.

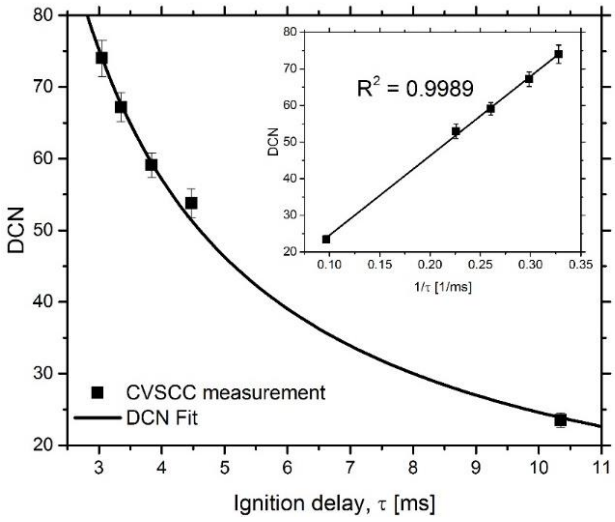

Fig. 2.8. Correlation between established DCNs for five pure fuel components and the CVSCC ignition delay times at ambient conditions of air at 818 K and 2.14 MPa.

3. Results and Discussion

3.1. Shock tube ignition delay

In this project ignition delay times have been measured using the reflected shock method for small alkenes [J9, J11] found as intermediates during the oxidation of larger paraffins, a series of n- and iso-alkanes [J3, J10, J16, J20] and large alkenes (decenes) [J2], and several multi-component jet fuels [J1, J22].

3.1.1. Small alkenes

Wide ranging studies of propene [J11] and isobutene [J9] autoignition (1-50 atm, 650-1700 K) have been carried out in collaboration with other shock tube (RPI, NUI Galway, Texas A&M, Stanford, and KAUST) and rapid compression machine (NUI Galway and University of Connecticut) groups. These data were used to improve the base small hydrocarbon kinetic mechanisms on which higher hydrocarbon kinetic models are developed and also provided direct comparisons of results from different shock tubes to ascertain reproducibility and uncertainty. The results from the different shock tubes exhibit good agreement. Experiments from common mixtures from the various facilities are within 20% of each other, Fig. 3.1. Best fits to ignition delay time measurements from individual shock tube facilities, illustrating the repeatability of measurements made in a single facility, exhibit 1σ scatter about those best fits of ±5–10% in all cases, well within the cited uncertainties for shock tube ignition delay (±15–20%) which take into account estimates of systematic uncertainties that potentially do not contribute to statistical scatter (e.g., systematic errors in calculated post-shock

conditions). Best fits to compilations of ignition delay data from shock tube experiments carried out at common conditions independently in multiple facilities, Fig. 3.1, show 1σ scatter ranging from ±10% to ±15%. This suggests that ±20–30% can be viewed as a metric for the reproducibility, the expected difference (with 95% confidence) between single independent measurements carried out in different laboratories, of high-temperature shock tube ignition delay measurements both here and generally. These wide ranging comparisons are to the PI's knowledge the first of their kind for shock tubes and illustrate the quality of the experiments results obtained from these facilities.

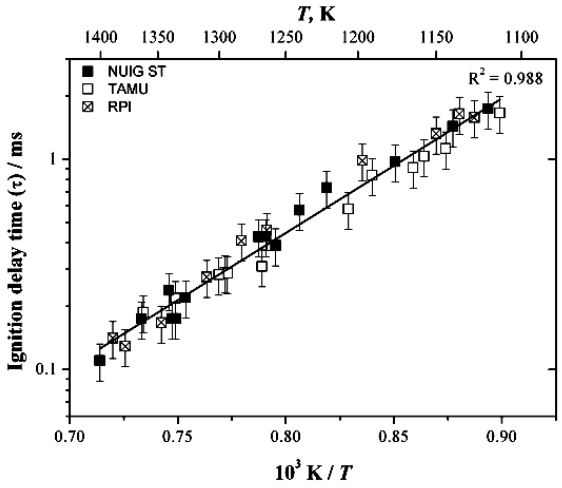

Fig. 3.1. Comparison of propene/air (φ = 1, 10 atm) ignition delay times in RPI, NUI Galway, and Texas A&M shock tubes.

3.1.2. Alkanes

A series of ignition delay studies were carried out for C_8 alkanes to determine the influence of branching on reactivity. N-Octane [13], 2-methylheptane [13], 3-methylheptane [J20], and 2,5-dimethylheptane [J16] were considered in mixtures with air at 20-50 atm, 650-1250 K, and φ = 0.5-2. These measurements quantify the influence of branching on paraffinic reactivity, a critical target for the development of kinetic models for high molecular weight alkanes found in large quantities in jet fuels. A subset of the ignition delay data is shown in Fig. 3.2 for the four isomers for a common pressure and mixture.

At high temperatures, ignition delay times for these four C8 isomers are indistinguishable due to the similarity of intermediates formed via beta scission of the alkyl radicals formed by H-atom abstraction and unimolecular decomposition of the C8 isomers. While at NTC and low temperatures, the ignition delay times for the four isomers deviate according to their DCNs or research octane numbers. Kinetic modeling is shown to quantitatively capture the reactivity differences for these isomers [13, J16, J20]. The differences between the branched compounds and n-octane can be attributed to the influence of the methyl substitutions on the rates isomerizations of OOQOOH radicals that lead to low-temperature chain branching. The deviation in NTC and low-temperature reactivity for 2,5-dimethylheptane, 3-methylheptane, 2-methylheptane are primarily attributed to differences in the competition between low-temperature chain branching and propagation pathways (i.e., cyclic ether formation and HO_2 elimination causing alkene formation).

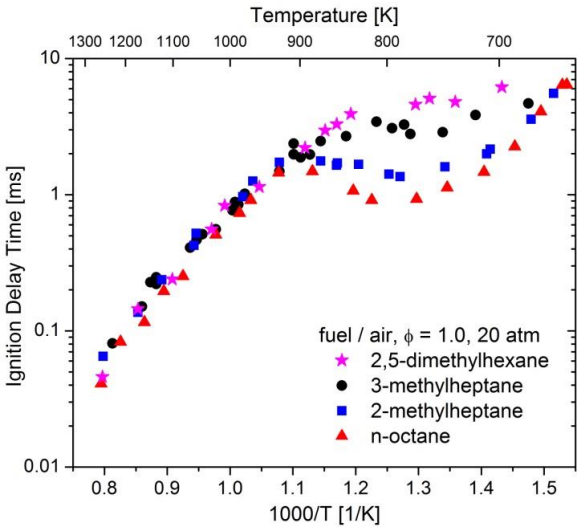

Fig. 3.2. Ignition delay comparisons for C8 alkane isomers.

Ignition delay time measurements have also been made for n-dodecane at extreme pressure conditions relevant to high pressure ratio engines and specifically those found in the Engine Combustion Network Sandia Spray A experiments. The shock tube studies were carried out for n-dodecane/air mixtures at equivalence ratios of 1.0 and 2.0 for nominal pressures of 40, 60, and 80 atm and also at 60 atm for stoichiometric n-dodecane/O_2/N_2 mixtures containing 13% and 15% O_2, to emulate reduced-O_2 mixtures containing exhaust gases. The parameter space spans the low-temperature, negative-temperature-coefficient, and high-temperature regimes (774-1163 K), providing characterization of the complex temperature dependence of ignition important in low-temperature combustion processes and the pressure and oxygen concentration dependencies across the three kinetic regimes. The measurements are compared *a priori* to several recently developed reduced kinetic models [14-17] with experiment-modeling deviations near the experimental uncertainties (20% in ignition delay) in several cases (Narayanaswamy et al. [16] and Wang et al. [17]). To our knowledge, these experiments represent the first gas-phase homogenous autoignition measurements made for n-dodecane at the extremely high-pressure conditions found in Spray A and provide critical targets for reduced models used in CFD simulations of that system. Comparison of several reduced n-dodecane models with experimental results are shown in Fig. 3.3. Note that at the high pressures encountered, the ignition delay in the NTC approaches 100 μs, a fraction of the residence time in a gas turbine combustor and indicative that low-temperature and NTC chemistry could be important in these environments.

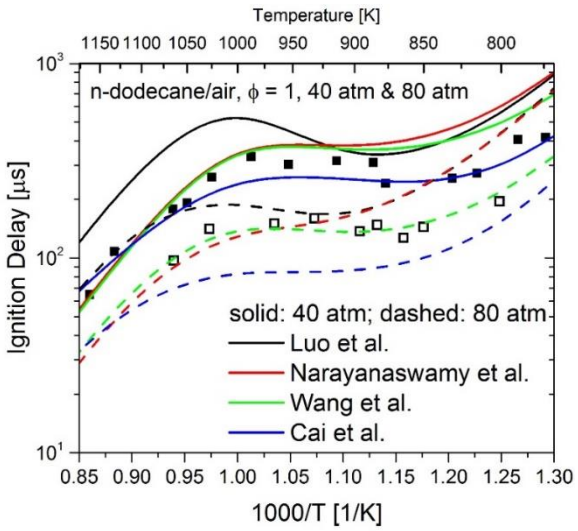

Fig. 3.3. Comparison of 40 atm and 80 atm ignition delay measurements with kinetic modeling predictions [14-17].

3.1.3. Alkenes vs alkanes

Similar comparative studies were performed for C10 species with and without double bonds. Ignition delay measurements were made for n-decane, 1-decene, and 5-decene mixtures in air at 20-40 atm, 650-1300 K, and φ=0.5-1.5. Example comparative ignition delay results are shown at common mixtures and pressure conditions in Fig. 3.4. An interesting inversion in reactivity can be observed between the compounds as temperature increases. In high-temperature region (T > 950 K), 1-decene displays very similar ignition delay time to n-decane and 5-decene has ignition delay consistently shorter than that of 1-decene and n-decane. In a low-temperature region (T < 950K), 5-decene shows significantly longer ignition delay than that of 1-decene and n-decane and 1-decene has a slightly longer ignition delay than n-decane.

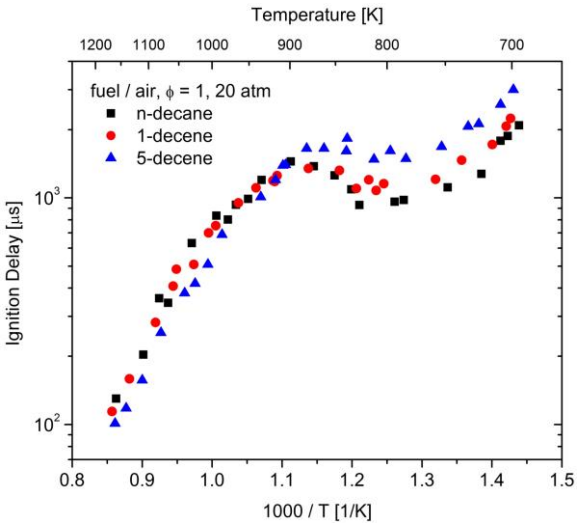

Fig. 3.4. Comparison of n-decene and n-decane ignition delay times.

It also evident that the low-temperature reactivity was much more significantly affected by the double bond position than high-temperature reactivity.

Previous work on n-alkenes [18] suggests that the dependence of the low-temperature reactivity of double bond location is governed by competition between chain branching through the conventional mechanism involving two molecular oxygen additions and the inhibitive direct elimination of HO_2 from ROO and Waddington mechanism, both of which increase in rate with a reduction in saturated alkyl chain length. At high-temperature, however, the double bonds increase the rate of fuel fragmentation due to the introduction of weaker allylic C-H bonds in 1- and 5-decene relative to the aliphatic bonds present in n-decane, allowing faster rates for H abstraction from the fuel, the primary initiation mechanism. 5-Decene is more reactive at higher temperatures than 1-decene, owing to the fact the double bond in the center of the carbon chain in 5-decene results in the modification of twice the number of secondary aliphatic C-H bonds found in n-decane to allylic C-H bonds as are modified in 1-decene. These ignition delay times will be valuable for the future development of kinetic models for unsaturated species and for aliphatic fuels where high molecular weight alkenes are found as intermediates in both high- and low-temperature combustion.

3.1.4. Jet Fuels

A large series of ignition delay time measurements have been made for Air Force relevant fuels [J1, J22] at conditions from 20-80 atm, 650-1400 K, and fuel/air at φ=0.5-2. Fuels considered include an average Jet A with and without the JP-8 additives [J22]; Fischer Tropsch fuels S-8, Shell GTL, and Sasol IPK [J22]; the Category A (1,2,3) JP-8 fuels [J1]; and the Gevo ATJ fuel [J10]. These studies provide a parametric evaluation of the influence of pressure, temperature, equivalence ratio, and molecular structure/fuel mixture on ignition delay. The important conclusions of this work are: 1) jet fuel ignition variability in the high-temperature region is extremely weak, while jet fuel ignition variability in the NTC and ow-temperature region is strong and correlates well with DCN; 2) the dependence of ignition delay on pressure and equivalence ratio can be described using power law scaling but the condition dependencies are much stronger in the NTC and low-temperature regions than at high-temperature; 3) ignition delay times at conditions of 800-1000 K and high pressures, critical as inlet conditions for gas turbine combustors are in the range of 0.1-3 ms, timescales that at their shortest approach mixing timescales indicating that under some gas turbine conditions low-temperature and NTC chemistry may play an important role. Example ignition delay times for a range of jet fuels are shown in Fig. 3.5 as is the dependence of ignition delay at the minima in the NTC on DCN.

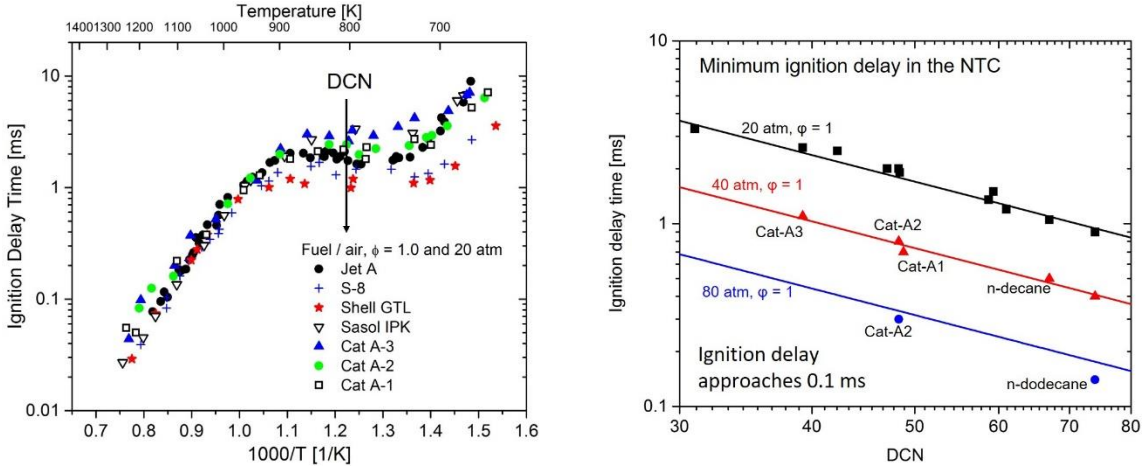

Fig. 3.5. Ignition delay times for Air Force jet fuels at fuel/air φ = 1 and 20 atm conditions (left); relationship between minimum ignition delay in the NTC (~800 K) and DCN (right).

3.2. Ignition delay models

While increasing computational power is allowing for the inclusion of a growing number of chemical reactions in combustion computational fluid dynamics (CFD) simulations, the high computational cost of chemical kinetic models for the combustion of large pure component fuels or multi-component mixtures restricts or prevents their use in CFD. Hence, there is need for reduced models that greatly simplify combustion chemistry while retaining reasonable predictability for use in CFD simulations of complex turbulent and sometimes multi-phase combustion phenomena. Of interest is the use of reduced reaction schemes for the prediction of autoignition. Models that capture the influence of fuel variability on combustion chemistry and autoignition are needed to predict fuel influence on engine operation and performance via CFD calculations. In this work we have developed two empirical approaches to describing ignition delay. The first is a correlative three-Arrhenius model that defines time scales for ignition in the three temperature regimes of interest: low, intermediate (NTC), and high temperature. The second is a generic and global seven-step reduced reaction model. Both of these models incorporate fuel variability through the inclusion of DCN as an input parameter.

3.2.1 Three-Arrhenius model

The similarity of high-temperature ignition delay time observed for a diverse range fuels and the simple dependence of ignition delay time on DCN, as shown in Fig. 3.5, motivates a pragmatic empirical model for ignition delay time based on a slight modification to the three-Arrhenius model of Weisser [19] and also utilized by Vandersickel et al. [20]. The Weisser model defines three time constants for low-, moderate-, and high-temperature oxidation. The overall ignition time at any temperature is expressed as a combination of those three time constants:

$$\frac{1}{\tau} = \frac{1}{\tau_L + \tau_M} + \frac{1}{\tau_H}$$

where τ is the ignition time and τ_L, τ_M, and τ_H the time constants for low-, moderate-, and high-temperature chemistry, respectively. See Fig. 3.6 for a graphical description of the model.

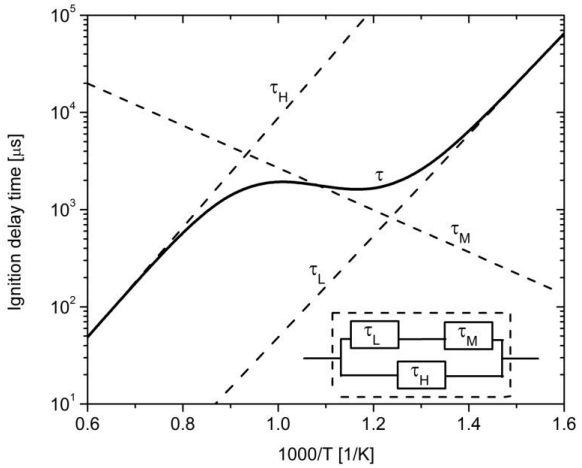

Fig. 3.6. Three-Arrhenius model for ignition delay time.

The three-Arrhenius model time constants can be expressed with Arrhenius temperature dependence and power-law functions for pressure, equivalence ratio, and DCN dependence, where incorporating DCN functionality to describe ignition delay time dependence on fuel variability is the unique contribution of the present work:

$$\tau_i = A_i \left(\frac{P}{P_{ref}}\right)^{\alpha_i} \phi^{\beta_i} \left(\frac{DCN}{DCN_{ref}}\right)^{\gamma_i} \exp\left(\frac{T_{act,i}}{T}\right) \text{ for } i = L, M, H$$

P_{ref} and DCN_{ref} are a reference pressure and reference DCN, and A_i, α_i, β_i, γ_i, and $T_{act,i}$ are chosen for each temperature range to fit experimental data. The model constants were adjusted to best fit a target database of measurements carried out in our laboratory for diesel and jet fuels, representing a range of experimental conditions relevant to engines: DCN = 31-80, ϕ = 0.25-1.5, P = 8-40 atm, and T = 650-1300 K. The best-fit model parameters are given in Gowdagiri et al. [J15].

Example comparisons between the three-Arrhenius model and the target jet fuel experimental ignition delay time data are given in Fig 3.7. (left), exhibiting relatively good agreement that is characterized for the entire target database in Fig. 3.7 (right). The standard deviation (1σ) for the

dispersion between experimental data and the three-Arrhenius model is ±20% of ignition delay time. The ignition delay time measurements show shot-to-shot scatter (reproducibility) of around ±10% (1σ) and we estimate their uncertainty at ±25% (2σ confidence interval) based on an analysis of the potential systematic uncertainties. Hence, the present three-Arrhenius model is predictive to within about twice the experimental uncertainty limits for a 2σ confidence interval; i.e., the 2σ (95%) confidence interval for experimental uncertainty is ±25% and 2σ model-experiment correlation is ±40%. As this suggests, the three-Arrhenius model provides a first-order description of the dependence of ignition delay time on conditions and DCN, chosen to represent fuel variability, but does not capture all the complexities of fuel chemistry. However, it is predictive to within the limits of most *a priori* kinetic modeling studies found in the literature and provides a simple way of predicting fuel global reactivity for different fuels with known DCNs and for differing conditions.

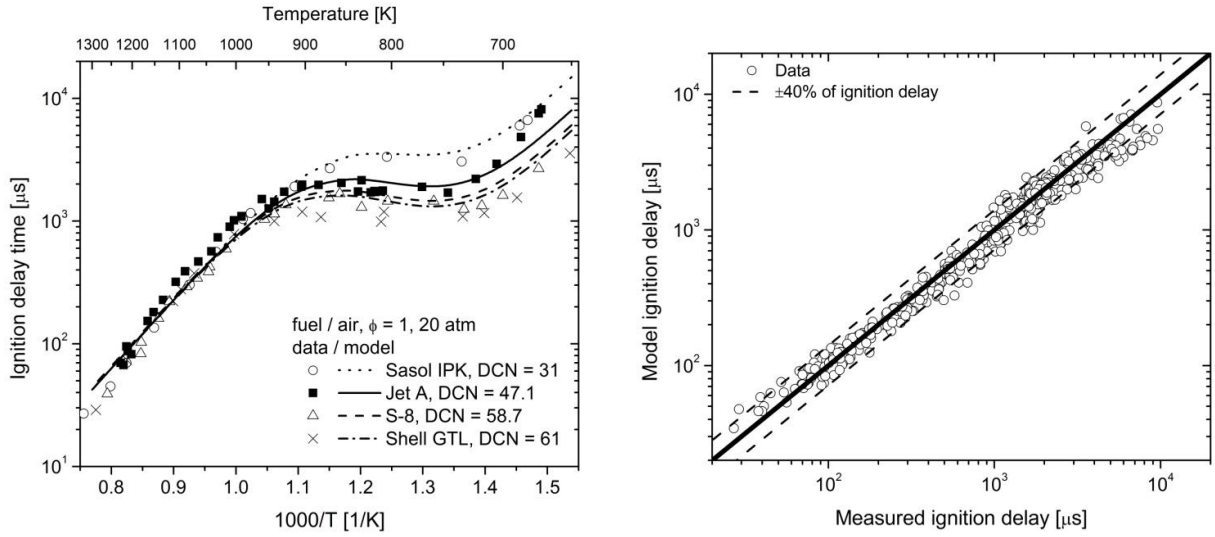

Fig. 3.7. Comparison of example jet fuel ignition delay time measurements with three-Arrhenius model (left); global model performance (right).

3.2.2 Global reduced model

A global reduced model was developed in this project as described by Gowdagiri et al. [J14]. It is a seven-step global reduced reaction model based on modification of the model of Zheng et al. [21]. The model is optimized to best predict shock tube ignition delay measurements carried out over a large range of conditions for jet and diesel fuels with a large range of reactivity, represented through the derived cetane number (DCN). The Zheng et al. model is a reduced model that uses composite chemical kinetic steps or quasi-global reactions to represent reaction progress from fuel and oxidizer to major products. The composite reaction steps represent classes and/or sequences of reactions that carry reaction flux under high-temperature or low-temperature oxidation conditions.

The reduced model is given in Table 3.1 for a generic C_mH_n hydrocarbon fuel. It is comprised of seven generic reaction steps that provide atom conservation and allow for radical branching and its inhibition in different temperature regimes. The model embodies high-temperature (> 1100 K) oxidation and ignition using two reaction steps, reactions (1) and (2). Reaction (1) describes fuel oxidation to H_2O and CO, the global rate of which is governed by $H+O_2 \rightarrow OH+O$ at high temperatures, the rate limiting chain branching reaction for high-temperature hydrocarbon oxidation and ignition. Reaction (2) then describes the oxidation of CO to CO_2. For the purposes of the present study, the pre-exponential A-factor and activation energy of reaction (1) were adjusted to best fit the shock tube high-temperature ignition delay within the target data set. While the rate parameters for reaction (2) were taken from Zheng et al. [21].

At low and intermediate temperatures, oxidation and autoignition is embodied within the reduced model in reactions (3) – (7). Low-temperature radical branching is initiated by the addition of molecular oxygen to a parent fuel radical, $R + O_2 \leftrightarrow RO_2$. In the case of alkane fuels, this is the addition of O_2 to an alkyl radical. $R + O_2 \leftrightarrow RO_2$ can be followed by isomerization, $RO_2 \leftrightarrow QOOH$, and the addition of another O_2, $QOOH + O_2 \leftrightarrow OOQOOH$. This reaction sequence is represented in the reduced model by reaction (3), $C_mH_n + 2O_2 \leftrightarrow I_1$, allowing for two oxygen additions to the fuel to produce an oxygenated radical intermediate, I_1. Reaction (3) is allowed to proceed in reverse to represent inhibitive (radical propagation) steps that reduce the reaction flux through the low-temperature radical branching sequence, including HO_2 elimination from RO_2 and QOOH, cyclic ether formation from QOOH, beta-scission of QOOH, and RO_2 dissociation back to $R + O_2$. Under the reduced model, autoignition in the NTC and low-temperature regions is highly sensitive to the rate parameters for reaction (3); hence, the forward and reverse A-factors for reaction (3) were adjusted to best fit experimental target data.

The oxygenated radical produced in reaction (3), I_1, can react to produce chain-propagating radicals, Y, in reaction (4). Y can then react with fuel and O_2 in reaction (5) to produce H_2O and CO, resulting in heat release. Hence, low- to intermediate-temperature first-stage ignition is controlled by reactions (4) and (5) and their competition with reverse reaction (3). The intermediate oxygenated radical, I_1, can also react via reaction (6) to form another branching agent, I_2, which can react in reaction (7) to produce radicals, Y. This reaction sequence is representative of the buildup of H_2O_2, embodied in I_2, and its dissociation to produce OH radicals, embodied in Y. These steps reduce degenerate radical branching through their competition with reaction (4), govern second-stage ignition, and control the turnover from the NTC regime to high-temperature ignition behavior. The major contribution of the work of Zheng et al. [21] was the addition of reactions (6) to (7) to the Schreiber et al. [22] model allowing for a better representation of NTC behavior. Reaction rate expressions for the seven-step model are given in Table 3.1. Thermodynamic data for the species can be found in [J14].

Table 3.1. Reduced global reaction model from Zheng et al. [21]. Parameters have been optimized in the present study. Reaction rate coefficients given by $k = A \exp(-E/RT)$ [units: cal, K, mol, cm^3, s].

Reaction		**A**	**E [cal mol^{-1}]**	**Reaction rate [mol cm^{-3} s^{-1}]**
(1)	$C_mH_n + (0.5m+0.25n)O_2 \rightarrow (0.5n)H_2O + mCO$	$A_{1,f}^{\ddagger} = 2.55\times10^{11}$	$E_{1,f}^{\ddagger} = 34740$	$k_{1,f}[C_mH_n]^{0.25}[O_2]^{1.5}$
(2)	$CO + 0.5O_2 \leftrightarrow CO_2$	$A_{2,f}^{*}= 1\times10^{14}$ $A_{2,r}^{*} = 1.2\times10^{7}$	$E_{2,f}^{*} = 40000$ $E_{2,r}^{*} = 40000$	$k_{2,f}[CO][H_2O]^{0.5}[O_2]^{0.25} -$ $k_{2,r}[CO_2]$
(3)	$C_mH_n + 2O_2 \leftrightarrow I_1$	$A_{3,f}^{\ddagger} = 9.48\times10^{19}\ P^{-2.2}\ DCN^2$ $A_{3,r}^{\ddagger} = 1.38\times10^{35}\ P^{-3.5}$ (P in atm)	$E_{3,f}^{*} = 37620$ $E_{3,r}^{*} = 88110$	$k_{3,f}[C_mH_n][O_2][M] - k_{3,r}[I_1]$
(4)	$I_1 \rightarrow 2Y$	$A_{4,f}^{\ddagger} = 1.2\times10^{6}$	$E_{4,f}^{*} = 3960$	$k_{4,f}[I_1]$
(5)	$Y + 0.5C_mH_n + (0.5m+0.25n-1)O_2 \rightarrow (0.5n)H_2O + mCO$	$A_{5,f}^{\ddagger} = 1\times10^{18}\ DCN^{0.25}$	$E_{5,f}^{*} = 32670$	$k_{5,f}[C_mH_n][Y]$
(6)	$I_1 \rightarrow I_2$	$A_{6,f}^{\ddagger} = 4.23\times10^{10}$	$E_{6,f}^{*} = 13860$	$k_{6,f}[I_1]$
(7)	$I_2 \rightarrow 2Y$	$A_{7,f}^{\ddagger} = 1\times10^{24}$	$E_{7,f}^{*} = 53460$	$k_{7,f}[I_2][M]$

*from Zheng et al. [20]; ‡optimized in present study

Rate parameters within the reduced seven-step model were adjusted to best fit a target shock tube ignition delay data set, comprised of shock tube ignition delay data from experiments carried out in our laboratory for jet and diesel fuels. The best fit model was subsequently compared with data from other laboratories to ascertain the consistency of the model with other data sets and indirectly the consistencies of experiments from different laboratories. To describe the influence of fuel reactivity variability on autoignition, DCN was chosen as a single parameter to represent fuel

reactivity. The A-factors for reaction (3) in the forward direction and reaction (5) were modified to include DCN dependence. Reaction (3) in the forward direction is the pivotal step in the low-temperature chain branching sequence and inclusion of DCN dependence in the A-factor allows for a best fit of model-predicted NTC and low-temperature autoignition to the target data shown to be correlated with DCN. Reaction (5), which provides second stage ignition, has influence on NTC ignition and high-temperature transition. Inclusion of DCN dependence in the reaction (5) A-factor was found to improve model predictability in this region. To best fit the target data DCN dependence of $A_{f,3} \propto DCN^2$ and $A_{f,5} \propto DCN^{0.25}$ was chosen. Note, the fuel average molecular formula, C_mH_n, also influences ignition through the coefficients in reactions (1) and (5). High-temperature ignition for aliphatic or primarily aliphatic fuels are shown to be relatively insensitive to fuel structure or composition and DCN in the present study (see prior sections); hence, no DCN dependence was included in the high-temperature reaction sequence, reactions (1) and (2).

Starting with the original Zheng et al. model parameters, parameters were adjusted to best fit the target ignition delay data set. Reaction (1) was first adjusted manually to best fit high-temperature data (> 1100 K). Next the DCN dependence of reaction (3) in the forward direction and reaction (5) were assigned through an iterative manual fit of the DCN dependence of measured ignition delay for T < 900 K. Finally, A-factors for reactions (3) – (7) were manually optimized to minimize the global deviation between model and experimental data. The activation energies for reactions (2) – (7), the pressure dependence of the A-factors for reaction (3), and the A-factors for reaction (2) were left unchanged from the values assigned by Zheng et al. [21].

Example comparisons of the model to the target shock tube ignition delay and global model performance is shown in Fig. 3.8. The comparison is globally very good with the model generally predicting ignition delay within the ±25% experimental uncertainty (2σ confidence interval) in measured ignition delay and capturing the ignition delay dependence on DCN, temperature, pressure, and equivalence ratio.

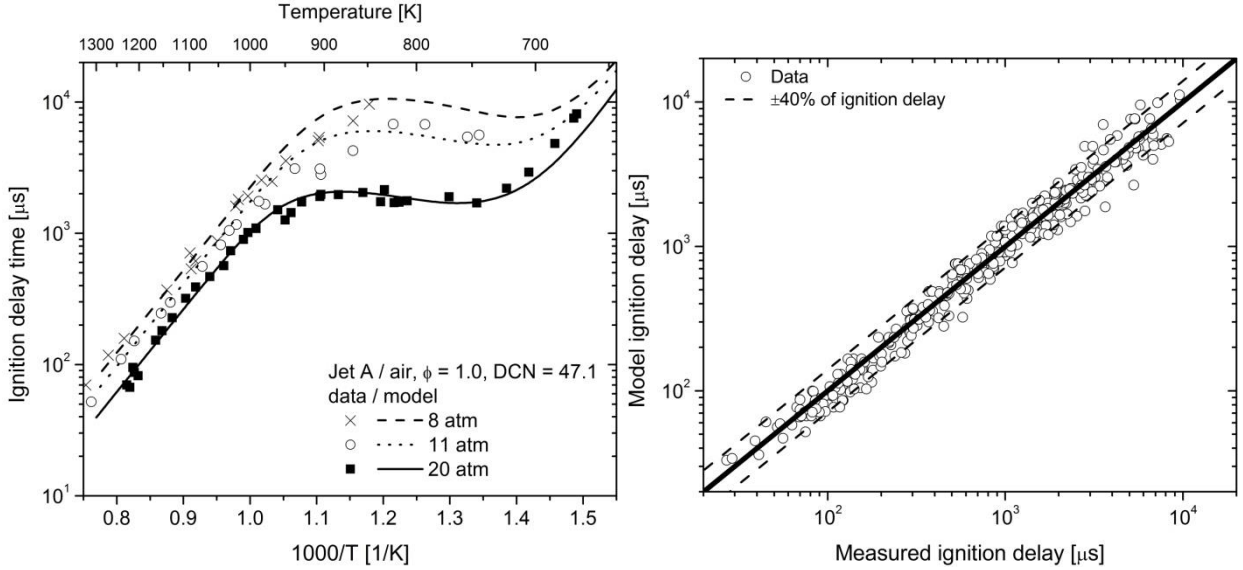

Fig. 3.8. Comparison of reduced global model with shock tube ignition delay measurements for Jet A (right) and global model performance (right).

3.3. CO formation during n-alkane oxidation

Carbon monoxide measurements were made during the dilute oxidation (0.5% and 5% O_2 in argon) of n-alkanes (n-heptane, n-decane, and n-dodecane) in both an intermediate temperature range (1121-1290) and a low-temperature range (686-797) [J5]. These measurements provide insight into

the pre-ignition reactivity and heat release rate, critical for the constraint of kinetic models such that they adequately capture low- to intermediate-temperature reactivity timescales.

Intermediate-temperature n-heptane experiments are shown in Fig. 3.9 with comparison to three independently-constructed detailed kinetic models commonly used throughout the literature: the comprehensive Lawrence Livermore National Laboratory (LLNL) model for n-alkanes reported by Sarathy et al. [23], the n-alkane model of Ranzi et al. [24] (Milano) which contains a lumped description of fuel fragmentation and early oxidation reaction pathways, and the JetSurf 2.0 model of Wang et al. [25] which contains a comprehensive treatment of high-temperature chemistry but does not include low-temperature pathways. All modeling calculations were performed under assumed constraints that best replicate the experimental conditions. The non-reacting pressure behind the reflected shock was assumed to vary according to measurement ($dP/dt = 2\%\ ms^{-1}$) and a contracting volume history was applied to provide that non-reacting pressure gradient [26]. Conservation of energy under the adiabatic assumption was solved for this contracting volume to determine the temperature variation due to both non-ideal gasdynamics and endothermic/exothermic chemistry. The Fig. 3.9 experimental results show an increased rate of CO formation with increasing temperature and experiment-model comparisons are consistent across the temperature space. The Milano model overpredicts the formation of CO, while the JetSurf model slightly underpredicts CO formation. The LLNL model predicts measurement very well up to 500 ppm of CO and after 500 ppm slightly underpredicts CO formation.

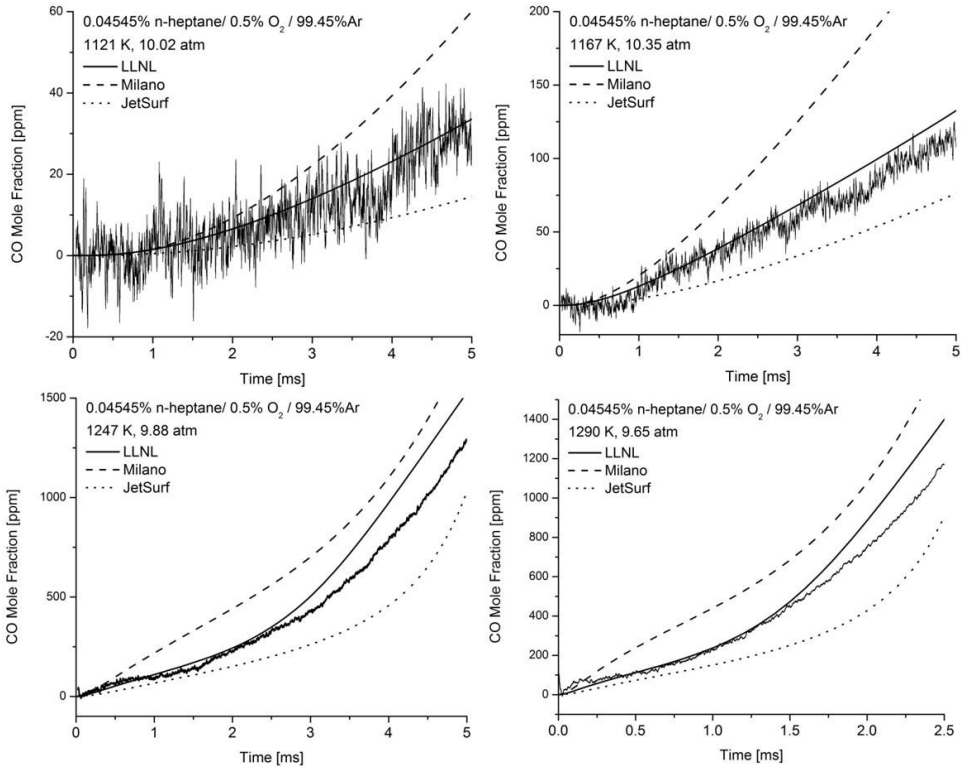

Fig. 3.9. Measured CO during the intermediate-temperature oxidation of 0.04545% n-heptane/0.5% O_2/Ar from 1121 to 1290 K with comparison to three kinetic models: LLNL [23], Milano [24], and JetSurf [25].

At the intermediate-temperature range exhibited in Fig. 3.9, according to the three chemical kinetics models considered, the n-alkanes are almost entirely consumed via H-atom abstraction by radicals. The resulting alkyl radicals then undergo beta-scission fragmentation reactions leading to a pool of CH_3, C_2H_4, C_3H_6, and H atoms. This intermediate pool then participates in a series of oxidation reactions which primarily progress through HCO to the measured CO. Eventually the CO would be

consumed in hot ignition and result in CO_2 formation; due to the dilute reactant mixture. Here, hot ignition is not reached in the available test time. Sensitivity analysis shows that the formation of CO is highly dependent to the rate coefficients for fuel fragmentation reactions, n-alkane decomposition and alkyl radical beta-scission, and the rate coefficient of the important high-temperature rate-limiting radical branching reaction, $H + O_2 \rightarrow OH + O$, which is responsible for the rate of radical production and thereby controls the rate of n-alkane consumption via H-abstraction by radicals.

Measurements of CO made under low-temperature conditions for n-heptane are shown in Fig. 3.10 with comparisons to the LLNL [23] and Milano [24] models, both of which contain low-temperature chemistry. The low-temperature CO measurements illustrate classic first-stage ignition behavior that can be explained by the low-temperature scheme [27]. Briefly, that scheme involves the n-alkane undergoing H-atom abstraction to form an alkyl radical that can add an O_2 ($R + O_2 \rightarrow RO_2$). The RO_2 can isomerize, through an internal H-atom transfer ($RO_2 \rightarrow QOOH$), after which a second O_2 addition can occur ($QOOH + O_2 \rightarrow OOQOOH$). Once OOQOOH is formed, it decomposes to ketohydroperoxide species and OH radicals. The ketohydroperoxide species further fragment leading ultimately to the formation of the measured CO. This is a chain branching sequence resulting in the formation of two OH radicals for every alkyl radical consumed and is responsible for first-stage ignition that is observed as low temperature heat release (LTHR) in internal combustion engine studies [28]. There are several chain propagating pathways that inhibit first-stage ignition and whose importance increases with increasing temperature, including direct HO_2 elimination from RO_2 and decomposition of QOOH to form an alkene or cyclic ether. The temperature dependence of the competition between the chain branching and the inhibitive chain propagation pathways results in negative-temperature coefficient (NTC) behavior.

The above described chemical pathways are exhibited in three features of the Fig. 3.10 results. First, following rapid CO formation due to first-stage ignition, the CO concentration comes to a plateau prior to complete fuel removal, due to the transition from chain branching to chain propagation as the temperature increases due to the exothermicity of first-stage oxidation. Similarly, the CO plateau concentration decreases with increasing initial temperature because less first-stage heat release is required for the transition from branching to propagation. Finally, the first-stage ignition delay decreases with increasing temperature up until approximately 760-780 K at which point the ignition becomes weaker and the first-stage ignition delay becomes longer (i.e., the entrance to the NTC is observed in the first-stage ignition delay, see Fig. 3.11). The modeling predictions for temperature rise indicate the temperature in the plateau following first-stage ignition is in the range from 800 to 840 K, depending on initial condition.

Here, we define the first-stage ignition delay based on the extrapolation of the maximum slope in measured CO concentration to the baseline (see upper left panel in Fig. 3.10). Sensitivity analysis for the important chemistry controlling first-stage ignition delay shows that the reaction sets within the low-temperature scheme govern ignition. Particularly important are the fate of the alkylperoxy (RO_2), hydroperoxyalkyl (QOOH), and hydroperoxyalkylperoxy (OOQOOH) radicals in controlling the duration of the first-stage ignition delay.

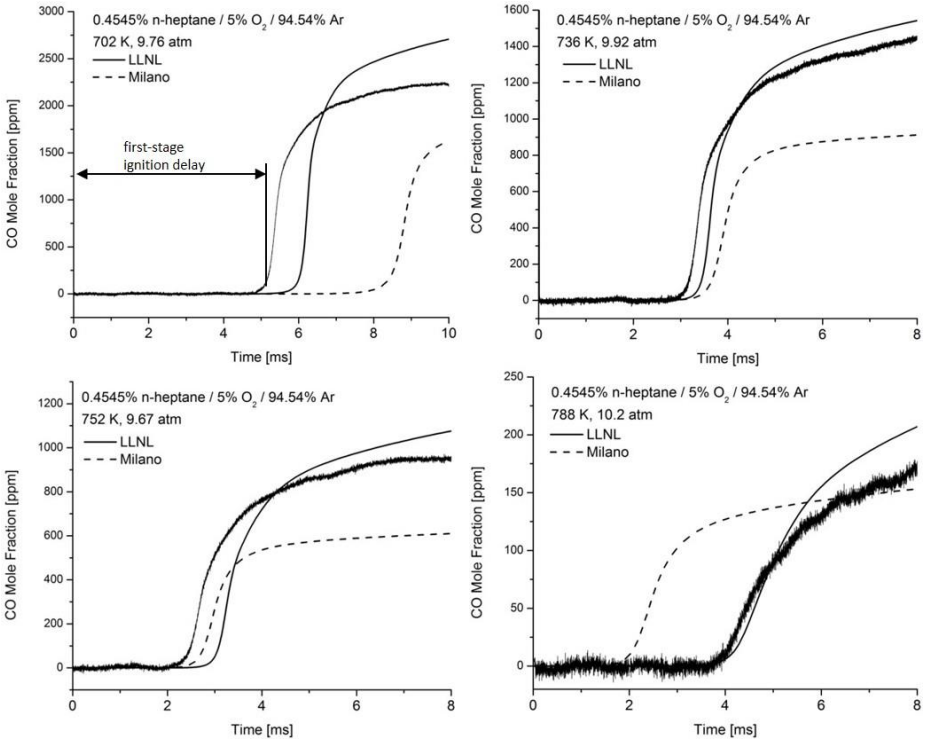

Fig. 3.10. Measured CO during the low-temperature oxidation of 0.4545% n-heptane/5% O_2/Ar from 702 to 788 K (measurement is solid black line with noise) with comparison to two kinetic models: LLNL [23] (solid line) and Milano [24] (dashed line).

Experiments were carried out near 10 atm for a range of temperatures and for n-heptane, n-decane, and n-dodecane. A comparison of CO measurements for the three fuels at a common condition (~750 K and ~10 atm) is shown in Fig. 3.11. The first-stage ignition delay time was found to decrease and the CO plateau mole fraction to increase with increasing n-alkane chain length. The first-stage ignition delay times are shown in Fig. 3.11 alongside the LLNL and Milano models for comparison. Both models are in reasonable agreement for first-stage ignition delay. We estimate first-stage ignition delay uncertainty at ±15% with primary contribution being temperature uncertainty.

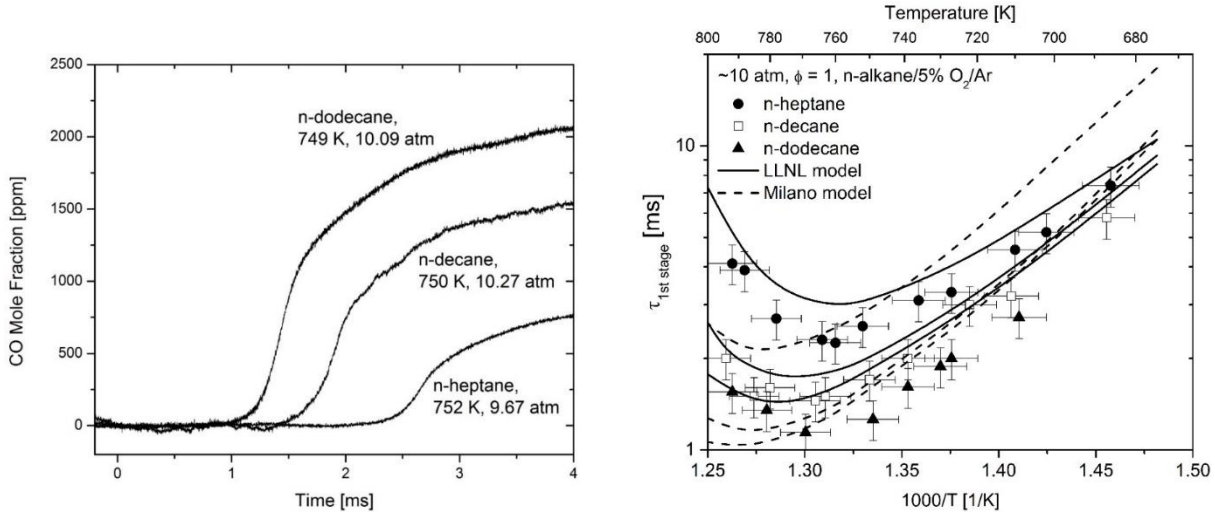

Fig. 3.11. Measured CO during the low-temperature stoichiometric oxidation of n-heptane, n-decane, and n-dodecane in 5% O_2/Ar around 750 K and 10 atm (left) and first-stage ignition delay times for range of temperatures (right).

The first-stage ignition delay times in Fig. 3.11 exhibit minima around 760-770 K. The ignition delay at this minima is found to exhibit simple power-law correlation with DCNs for these compounds [29]. The DCN, measured in a spray combustion apparatus under similar low-temperature conditions, indicates the relative low-temperature reactivity of fuels but is also complicated by a multitude of physical and chemical effects found in spray combustion. The correlation between this fundamental shock tube measurement for first-stage ignition delay, measured using a sensitive laser-based approach under dilute homogenous gas-phase conditions, and DCN, an engineering parameter measured under multiphase turbulent conditions, suggests that ignition timing in low-temperature internal combustion engines may often be controlled by chemistry and indicates the importance of homogenous reactor kinetic studies and low-temperature kinetic model development. This finding also motivates the study of spray ignition under kinetically-limited conditions, as described in the following section.

3.4. Spray ignition

Spray ignition studies have been carried out for alkanes (normal, branched, and cyclic) and alkylbenzenes and blends of alkylbenzenes with n-alkanes as described in the works of Tekawade et al. [J4, J6]. These experiments were performed in the CVSCC and provided quantitative spray ignition delay times across a range of temperature and pressure and DCN determinations. These experiments provide understanding of relative fuel reactivity, reactivity blending rules, and targets for future reacting flow simulations. The major findings of these studies are summarized here.

3.4.1. Alkanes

Spray ignition studies for alkanes were performed at wide ranging conditions across the low-temperature combustion regime (1-4 MPa, 650-825 K) and for n-alkanes (C7-C16); iso-octane, iso-cetane, and 2,6,10-trimethyldodecane; and cyclohexane and methylcyclohexane. Spray ignition delay times for these conditions and fuels range from 2 to 300 ms, providing determination of the influence of molecular structure, pressure, and temperature on both first-stage and total ignition delay. An example of the influence of molecular structure is exhibited in Fig. 3.12 where a variation in spray ignition delay for n-alkanes from n-heptane to n-hexadecane of around a factor of two is illustrated at a common pressure and across the low-temperature regime. The important global observations from this study on alkanes [J6] are:

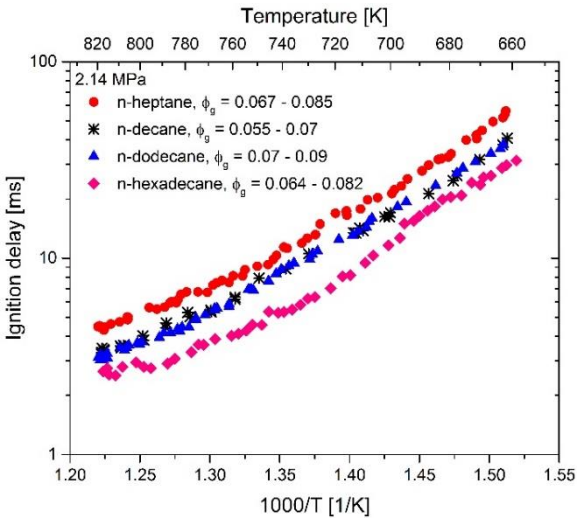

Fig. 3.12. N-Alkane spray ignition delay dependence on chain length (spray ignition in air at 2.14 MPa).

1) Two-stage ignition is most distinct for the iso-alkanes and the definition of ignition delay time is particularly important in these cases with prominent two-stage ignition.
2) Ignition delay decreases with increasing temperature but with reduction in apparent activation energy with increasing temperature from 750 to 825 K, indicative of negative-temperature-coefficient-like behavior.
3) Total ignition delay decreases with increasing n-alkane chain length according to $\tau \propto carbon\ number^{-0.7}$.

4) Total ignition delay decreases with increasing pressure with increased pressure dependence at higher temperature.
5) 2,6,10-trimethyldodecane has very similar spray ignition behavior to n-alkanes, indicating that n-alkanes can be used as surrogates for lightly branched alkanes in modeling and experiments.
6) Comparison of the CVSCC results with those from the Ignition Quality Tester (IQT) showed good agreement for fuels exhibiting nearly single-stage ignition. For low Derived Cetane Number (DCN) fuels (DCN < 20) exhibiting distinct two-stage ignition, ignition delay and DCN is extremely sensitive to the definition of the start of combustion and to experimental parameters. In these cases, consideration of the pressure or heat release history is important for understanding fuel reactivity.

3.4.2. Alkylbenzenes

Spray ignition studies for long-side-chain alkylbenzenes (n-octylbenzene and n-decylbenzene), compounds for which there are limited prior kinetic studies, were performed. The ignition delay for these neat compounds were compared against functional-group-equivalent blends of alkylbenzenes containing small substituted side chains (toluene or n-propylbenzene) and n-alkanes (n-heptane or n-decane). These comparisons revealed that the functional-group-equivalent blends have lower reactivity than the long-side-chain alkylbenzenes (n-octylbenzene and n-decylbenzene). For example, see Fig. 3.13 spray ignition delay comparisons of n-decylbenzene results with n-propylbenzene/n-heptane and toluene/n-decane where the spray ignition delay times for n-decylbenzene are appreciably shorter than those for equivalent toluene/n-decane and n-propylbenzene/n-heptane blends.

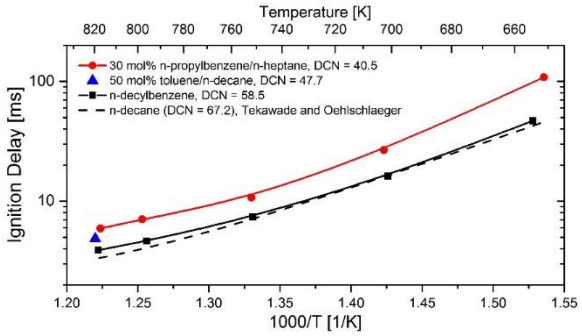

Fig. 3.13. Spray ignition delay measurements for n-decylbenzene with comparison to n-alkylbenzene/n-alkane blends. Injection is into air at an initial pressure of 2.14 MPa and initial temperatures from 650 to 820 K.

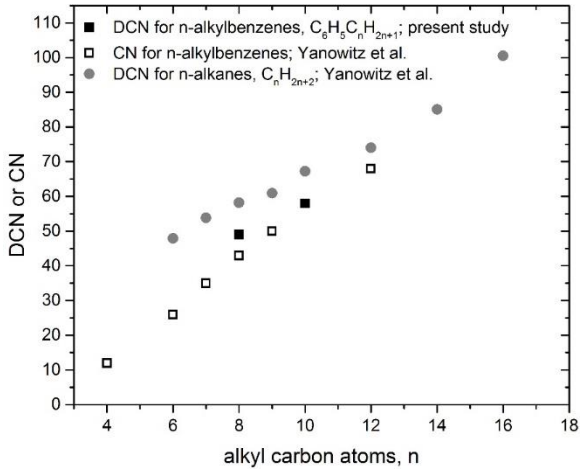

Fig. 3.14. DCN/CN measurements for n-alkylbenzenes and n-alkanes as a function of alkyl carbon atoms.

The observation that n-decylbenzene and n-octylbenzene have greater reactivity than surrogates comprised of smaller n-alkylbenzenes and n-alkanes seeking to match functional groups, suggests that a synergistic reactivity promotion occurs when the aromatic ring has a long alkyl side chain substitution. The synergism occurs due to the weak benzylic C-H and C-C bonds that exist in n-alkylbenzenes and promote the formation of alkyl radicals, as explored in kinetic modeling studies n-propylbenzene and n-butylbenzene oxidation [30-32]. At the benzylic site within an alkylbenzene the C-H bond dissociation energy (BDE) is 86-87 kcal/mol [33], substantially weaker than a secondary aliphatic C-H bond (BDE = 98.6 kcal/mol [34]), and the benzylic C-C BDE is 76.7 kcal/mol [34], again much weaker than an aliphatic C-C bond (87-89 kcal/mol [34]. At the low

temperatures considered in the present study, the aromatic ring reacts at significantly longer time scales than the alkyl chain and the rate of reaction for the n-alkylbenzene is controlled by the formation of an alkyl radical from the side chain and the subsequent low-temperature radical chain branching process for that alkyl radical. The benzylic C-H bond in n-decylbenzene and n-octylbenzene leads to faster rates of H abstraction for these compounds relative to n-alkanes and faster rates for alkyl radical formation from the subsequent beta-scission fragmentation. While H abstraction is the primary mode of fuel consumption at the low temperatures considered, the weak benzylic C-C bond in the n-alkylbenzenes also increases the rate of alkyl radical formation. In the comparison of n-decylbenzene with n-decane and n-octylbenzene with n-heptane, the n-alkylbenzenes ultimately have longer ignition delay times because the low-temperature chain branching from the alkyl side chain must compete with radical scavenging by the aromatic ring. However, n-decylbenzene, n-octylbenzene, and the binary blends considered contain similar quantities of aromatic carbon and therefore should all have similar radical scavenging potential. In these cases, the rate of reaction should only differ based on the formation rate of alkyl radicals and we hypothesize that the weaker bond strengths in the large n-alkylbenzenes, leading to enhanced low-temperature reactivity, results in the observed greater reactivity of n-alkylbenzenes relative to functional-group-equivalent surrogates comprised of small alkylbenzenes and n-alkanes.

The finding that there is a synergism between the aromatic and alkyl functionalities in n-alkylbenzenes suggests that the DCNs for large n-alkylbenzenes should approach those of n-alkanes for extremely long n-alkylbenzene side chains. A comparison of the present DCN measurements with DCN and cetane number (CN) measurements from the literature indeed show this to be the case. See Fig. 3.14 for a comparison of DCNs for n-alkanes [29] with DCNs (present study) and CNs [29] for n-alkylbenzenes on the basis of number of alkyl carbon atoms. The deviation in DCN/CN for n-hexane vs n-hexylbenzene is large (22 units) while the deviation for n-dodecane vs n-dodecylbenzene is small (6 units). Additionally, Fig. 3.14 shows that the present DCN measurements for n-octylbenzene and n-decylbenzene are in reasonable agreement with prior CN measurements for n-alkylbenzenes.

3.4.3. Alkylbenzene/n-alkane blends

Studies of blends of alkylbenzenes (1,3,5-trimethylbenzene, n-propylbenzene, n-butylbenzene) with n-heptane and n-decane also reveal interesting mixing behavior between the alkyl and aromatic functionalities; see DCN determinations for example blends are in Fig. 3.14. The blends of C9-C10 alkylbenzenes in n-decane show reactivity trends across the concentration space that corroborates with the chemical kinetic reactivity of the respective pure alkylbenzenes with greater low- to moderate-temperature reactivity for longer alkyl side chains. Most interestingly, clearly linear blending rules for prediction of DCN do not hold for these mixtures comprised of components with vastly different reactivity. Within the literature several models have been developed to describe the nonlinear blending behavior of reactivity metrics (e.g., cetane number, octane number) [35-36] as observed in Fig. 3.14. Here we compare the nonlinear blending model of Ghosh and Jaffe [35], shown to provide accurate description of blending effects observed in gasoline primary reference fuels

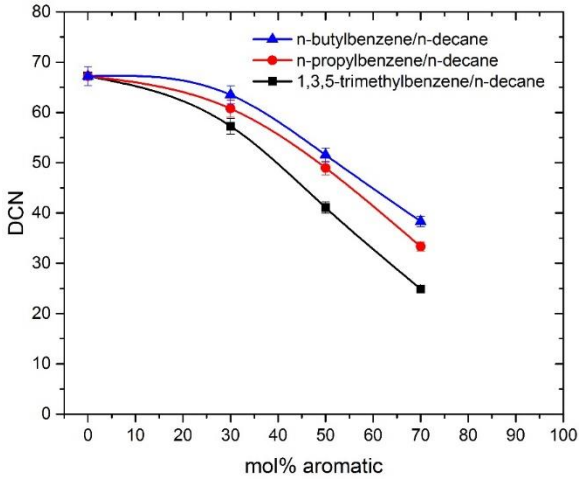

Fig. 3.14. DCN determinations for blends of C9-C10 alkylbenzenes in n-decane.

(PRFs) [37], and a new blending model we propose. The Ghosh and Jaffe model, written in terms of DCN and mole fraction of the each blend component, yields an expression for the DCN of a blend, DCN_{blend}, as follows: $DCN_{blend} = \frac{\sum X_i \beta_i DCN_i}{\sum X_i \beta_i}$, where in X_i is the mole fraction of each blend component, DCN_i the pure component DCN, and β_i an adjustable fitting parameter to describe component nonlinear blending contributions to DCN. As pointed out by Haas and Dryer [37], the values for β_i are only meaningful with respect to a reference; hence, in the below analysis we have chosen n-decane as the reference and $\beta_{n-decane}$ = 1. In Fig. 3.15 (top panel) we compare the Ghosh and Jaffe model with the present DCN measurements for n-propylbenzene/n-decane blends for variable $\beta_{n-propylbenzne}$. Our emphasis in this comparison is to not provide a best fit of the data but to illustrate the nonlinearity predicted by the Ghosh and Jaffe model. In these calculations we have fixed the DCNs for n-decane and n-propylbenzene at 67.2 and 10, respectively. In principle, the DCN for n-propylbenzene should also be adjustable, given it is uncertainty; however, its choice does not affect the shape of the DCN fall off curve and we found values for $DCN_{n-propylbenzene}$ from 0 to 15 do not appreciably influence the experiment-model comparison. Because the Ghosh and Jaffe model has fixed values for β_i across the blend space, the nonlinear contribution of each component is constant across the blend space and the model predicts a departure from linearity that is largest near the center that blend space. While the Ghosh and Jaffe model performs better than linear DCN blending, it appears to not adequately to capture the "shape" of the nonlinearity observed across the alkylbenzene/n-decane blend space as it always under predicts the DCN for blends containing 30 mol% aromatics and over predicts DCN for blends with 70 mol% aromatics. Hence, we seek to develop a model that better captures the apparent experimental trend.

DCN is a measure of reactivity; therefore, it is reasonable to consider DCN as an overall reaction rate with an apparent overall reaction order. For blends, the DCN could have different reaction orders with respect to concentrations of each component and the DCN of the blend would be the summation of each component contribution. Based on this hypothesis, the DCN of a blend could be written as: $DCN_{blend} = \frac{\sum X_i^{n_i} DCN_i}{\sum X_i^{n_i}}$, where now n_i is an adjustable parameter representing an overall reaction order for each species. Comparisons of this new proposed model to the n-propylbenzene/n-decane blend data are shown in Fig. 3.15 (middle panel) for variable n_i. A best fit is achieved for $n_{n-decane}$ = 1 and $n_{n-propylbenzene}$ = 2. Again, the DCNs for n-decane and n-propylbenzene are fixed at 67.2 and 10, respectively. Further comparisons of DCN data for alkylbenzenes/n-decane blends are illustrated in Fig. 3.15 (bottom panel) for $n_{n-decane}$ =1 and $n_{aromatic}$ =2 with good agreement for all three blending pairs. These best fit reaction orders for DCN would suggest a kinetic scenario, consistent with the kinetic modeling literature [38], in which aromatics rate limit blend reactivity due to

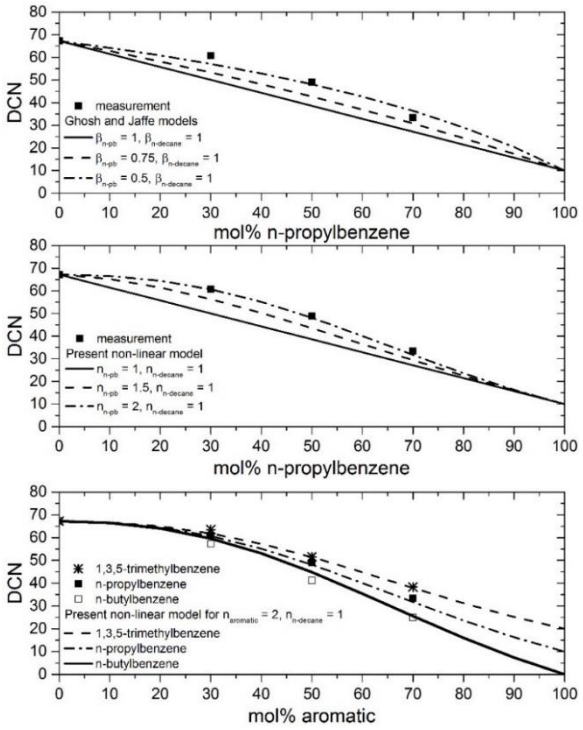

Fig. 3.15. Comparisons of nonlinear blending models for DCN with measurements for alkylbenzene/n-decane blends: Ghosh and Jaffe [35] (top); new nonlinear model for n-propylbenzene/n-decane (middle); new nonlinear model three aromatic/n-decane pairs (bottom).

bimolecular scavenging reactions (radical + aromatic → stables) and n-alkanes promote blend reactivity through the low-temperature chain branching sequence [38] that is rate limited by unimolecular isomerization reactions (e.g., isomerization of alkylperoxy radicals to alkyl hydroperoxyalkyl radicals, RO_2 → QOOH).

4. Conclusions

This project enabled a series of important experimental studies related to high molecular weight hydrocarbon combustion reactivity and ignition chemistry at high-pressure engine conditions across three temperature regimes of interests: high-, low-, and NTC-temperature regimes. The results produced in this project provides a rich database for future development of kinetic models and multi-physics reacting flow simulations. Several important conclusion of the present work are:

1) The high-temperature reactivity variability of jet fuels and components under engine conditions is modest.
2) The low-temperature and NTC reactivity variability of these fuels can be very large, factors of 2-3 to an order of magnitude variation in ignition delay for jet fuels.
3) The dependence of ignition delay on conditions and mixture is significantly stronger in the NTC and low-temperature regimes than at high temperatures.
4) Despite the thousands of elementary chemical reactions contributing to ignition chemistry of hydrocarbon fuels, ignition delay can be described with a relatively small number of parameters (dozens) either in correlative models or global reduced kinetic models.
5) Low- and intermediate-temperature heat release, prior to and during ignition, can be monitored using sensitive mid-infrared CO laser absorption, providing a new target for model development and understanding into two-stage ignition processes.
6) Spray ignition studies provide for the kinetic screening of fuels, or relative reactivity, and establish a target for reactive flow simulations. These studies also can provide characterization of non-linear reactivity mixing for mixtures comprised of high-reactivity alkanes and low-reactivity aromatics.

5. Participating Personnel

Principle Investigator
Prof. Matthew Oehlschlaeger

Graduate Students (partially supported by AFOSR funds)
Aniket Tekawade, Ph.D. candidate (expected May 2017)
Graham Kosiba, Ph.D. candidate (expected May 2017)
Chris Tilger, Ph.D. candidate (expected December 2016)
Mingdi Huang, (Ph.D. August 2015), "Computational Fluid Dynamics Studies of the Influence of Fuel Variability on Diesel Engine Operation."
William Gerken (Ph.D. May 2014, M.S. May 2013), "Nanofluid Droplet Evaporation," & "The Autoignition of Tetralin, an Endothermic Fuel," currently at United Launch Alliance, Centennial, CO.
Sandeep Gowdagiri (Ph.D. December 2014), "Fuel Autoignition Variability: Shock Tube Measurements, a Reduced Kinetic Model, and Diesel Engine Studies," currently at Ingersoll Rand, Tyler, TX.
Haowei Wang (Ph.D. May 2012), "Shock Tube Studies of the Autoignition of Jet Fuels, Surrogates, and Components," currently an Assistant Professor at California State University Fullerton.

Collaborators
Prof. Henry Curran, National University of Ireland, Galway
Prof. Frederick Dryer, Princeton University
Prof. Yiguang Ju, Princeton University
Prof. Tonghun Lee, University of Illinois
Dr. William Pitz, Lawrence Livermore National Laboratory
Prof. Mani Sarathy, KAUST
Prof. Jackie Sung, University of Connecticut
Dr. Charlie Westbrook, Lawrence Livermore National Laboratory

6. Journal Publications

J1. S. Burden, A. Tekawade, T.A. Deverter, G.J. Liskovich, "Spray and Shock Tube Ignition Studies of Jet Fuels," in preparation.

J2. A. Tekawade, T. Xie, M.A. Oehlschlaeger, "Comparative Study of the Ignition of Decenes and n-Decane: Spray and Shock Tube Experiments," in preparation.

J3. G.J. Liskovich, M.A. Oehlschlaeger, "Ignition Delay Measurements for n-Dodecane/N_2/Air Mixtures at High Pressures," in review.

J4. A. Tekawade, M.A. Oehlschlaeger, "Spray Ignition Experiments for Alkylbenzenes and Alkylbenzene/n-Alkane Blends," in review.

J5. A. Tekawade, G. Kosiba, M.A. Oehlschlaeger, "Time-Resolved Carbon Monoxide Measurements During the Low- to Intermediate-Temperature Oxidation of n-Heptane, n-Decane, and n-Dodecane," *Combustion and Flame*, 173, 402-410 (2016).

J6. A. Tekawade, M.A. Oehlschlaeger, "An Experimental Study on the Spray Ignition of Alkanes," *Fuel*, 185, 381-393 (2016).

J7. M. Huang, S. Gowdagiri, X.M. Cesari, M.A. Oehlschlaeger, "Diesel Engine CFD Simulations: Influence of Fuel Variability on Ignition Delay," *Fuel*, 181, 170-177 (2016).

J8. S.M. Sarathy, G. Kukkadapu, T. Javed, A. Ahmed, A. Tekawade, M. Mehl, G. Kosiba, S. Park, M. El Rachidi, W.L. Roberts, M.A. Oehlschlaeger, C.J. Sung, A. Farooq,

"Compositional Effects on the Ignition of FACE Gasolines," *Combustion and Flame*, 169, 171-193 (2016).

J9. C.W. Zhou, Y. Li, E. O'Connor, K.P. Somers, S. Thion, C. Keesee, O. Mathieu, E.L. Petersen, T.A. DeVerter, M.A. Oehlschlaeger, G. Kukkadapu, C.J. Sung, M. Alrefae, F. Khaled, A. Farooq, P. Dirrenberger, P.A. Glaude, F. Battin-Leclerc, J. Santer, Y. Ju, T. Held, F.M. Haas, F.L. Dryer, H.J. Curran, "A Comprehensive Experimental and Modeling Study of Isobutene Oxidation," *Combustion and Flame*, 167, 353-379 (2016).

J10. S.H. Won, F.M. Haas, A. Tekawade, G. Kosiba, M.A. Oehlschlaeger, S. Dooley, F.L. Dryer, "Combustion Characteristics of C4 iso-Alkane Oligomers: Experimental Characterization of iso-Dodecane as a Jet Fuel Surrogate Component," *Combustion and Flame*, 165, 137-143 (2016).

J11. S.M. Burke, U. Burke, R. McDonagh, O. Mathieu, E.L. Petersen, W. Wang, M.A. Oehlschlaeger, B. Rhodes, R.K. Hanson, D. Davidson, B.W. Weber, C.J. Sung, J. Santer, Y. Ju, E.N. Volkov, A.A. Konnov, M. Alrefae, F. Khaled, A. Farooq, H.J. Curran, "An Experimental and Modeling Study of Propene Oxidation. Part 2: Ignition Delay Times and Flame Speeds," *Combustion and Flame*, 162, 296-314 (2015).

J12. S.M. Sarathy, G. Kukkadapu, M. Mehl, W. Wang, T. Javed, S. Park, M.A. Oehlschlaeger, A. Farooq, W.J. Pitz, C.J. Sung, "Ignition of Alkane-Rich FACE Gasoline Fuels and their Surrogates," *Proceedings of the Combustion Institute*, 35, 249-257 (2015).

J13. S. Gowdagiri, X.M. Cesari, M. Huang, M.A. Oehlschlaeger, "A Diesel Engine Study of Conventional and Alternative Diesel and Jet Fuels: Ignition and Emissions Characteristics," *Fuel*, 136, 253-260 (2014).

J14. S. Gowdagiri, M.A. Oehlschlaeger, "A Global Reduced Model for Conventional and Alternative Jet and Diesel Fuel Autoignition," *Energy and Fuels*, 28, 2795-2801 (2014).

J15. S. Gowdagiri, W. Wang, M.A. Oehlschlaeger, "A Shock Tube Ignition Delay Study of Conventional Diesel Fuel and Hydroprocessed Renewable Diesel Fuel from Algal Oil," *Fuel*, 128, 21-29 (2014).

J16. S.M. Sarathy, T. Javed, F. Karsenty, A. Heufer, W. Wang, S. Park, A. Elwardany, A. Farooq, C.K. Westbrook, W.J. Pitz, M.A. Oehlschlaeger, G. Dayma, H.J. Curran, P. Dagaut, "Comprehensive Experimental and Kinetic Modeling Study of 2,5-Dimethylhexane, an Iso-Paraffinic Surrogate for Transportation Fuels," *Combustion and Flame*, 161, 1444-1459 (2014).

J17. S.H. Won, S. Dooley, P.S. Veloo, H. Wang, M.A. Oehlschlaeger, F.L. Dryer, Y. Ju, "The Combustion Properties of the Synthetic Diesel Fuel 2,6,10-Trimethyldodecane and a Molecular Analysis," *Combustion and Flame*, 161, 826-834 (2014).

J18. H. Wang, W.J. Gerken, W. Wang, M.A. Oehlschlaeger, "Experimental Study of the High-Temperature Autoignition of Tetralin," *Energy and Fuels*, 27, 5483-5487 (2013).

J19. P. Dievart, H.H. Kim, S.H. Won, Y. Ju, S. Dooley, F.L. Dryer, W. Wang, M.A. Oehlschlaeger, "The Combustion Properties of 1,3,5-Trimethylbenzene and a Kinetic Model," *Fuel*, 109, 125-136 (2013).

J20. W. Wang, Z. Li, M.A. Oehlschlaeger, D. Healy, H.J. Curran, S.M. Sarathy, M. Mehl, W.J. Pitz, C.K. Westbrook, "An Experimental and Modeling Study of the Autoignition of 3-Methylheptane," *Proceedings of the Combustion Institute*, 34, 335-343 (2013).

J21. S. Dooley, S.H. Won, S. Jahangirian, Y. Ju, F.L. Dryer, H. Wang, M.A. Oehlschlaeger, "The Combustion Kinetics of a Synthetic Paraffinic Jet Aviation Fuel and a Fundamentally Formulated, Experimentally Validated Surrogate Fuel," *Combustion and Flame*, 159, 3014-3020 (2012).

J22. H. Wang, M.A. Oehlschlaeger, “Autoignition Studies of Conventional and Fischer-Tropsch Jet Fuels,” *Fuel*, 98, 249-258 (2012).

7. Honors and Awards for PI

Fellow, American Society of Mechanical Engineers, 2015
Rensselaer, James M. Tien ’66 Early Career Award for Faculty, 2013
Rensselaer, MANE Strategic Advisory Council Classroom Excellence Award, 2013
Rensselaer, School of Engineering, Classroom Excellence Award, 2011
Society of Automotive Engineers (SAE), Ralph R. Teetor Educational Award, 2011

8. Interactions

During this project, the PI had interactions with Dr. J. Tim Edwards (AFRL) regarding the composition of traditional and alternative jet fuels; with Dr. Med Colket (United Technologies) regarding kinetics and conditions in gas turbines; with Dr. William Pitz (LLNL), Prof. Mani Sarathy (KAUST), and Prof. Henry Curran (NUI Galway) regarding the development of chemical kinetic models; and with Profs. Yiguang Ju (Princeton), Tonghun Lee (UIUC), and Jackie Sung (UConn) regarding experimental methods, comparisons, refinements, and uncertainties.

9. References

1. S.S. Vasu, D.F. Davidson, and R.K. Hanson, "Jet Fuel Ignition Delay Times: Shock Tube Experiments Over Wide Conditions and Surrogate Model Predictions," *Combustion and Flame*, 152, 125-143 (2008).
2. H.P.S. Shen, J. Steinberg, J. Vanderover, and M.A. Oehlschlaeger, "A Shock Tube Study of the Ignition of n-Heptane, n-Decane, n-Dodecane, and n-Tetradecane at Elevated Pressures," *Energy and Fuels*, 23, 2482-2489 (2009).
3. D.F. Davidson, D.R. Haylett, and R.K. Hanson, "Development of an Aerosol Shock Tube for Kinetic Studies of Low-Vapor-Pressure Fuels," *Combustion and Flame*, 155, 108-117 (2008).
4. H.P.S. Shen and M.A. Oehlschlaeger, "The autoignition of C8H10 aromatics at moderate temperatures and elevated pressures," *Combustion and Flame*, 156, 1053-1062 (2009).
5. W. Wang, S. Gowdagiri, and M.A. Oehlschlaeger, "The high-temperature autoignition of biodiesels and biodiesel components," *Combustion and Flame*, 161, 3014-3021 (2014).
6. J. Vanderover and M.A. Oehlschlaeger, "A mid-infrared scanned-wavelength laser absorption sensor for carbon monoxide and temperature measurements from 900 to 4000 K," *Applied Physics B*, 99, 353-362 (2010).
7. J. Vanderover, W. Wang, and M. A. Oehlschlaeger, "A carbon monoxide and thermometry sensor based on mid-IR quantum-cascade laser wavelength-modulation absorption spectroscopy," *Applied Physics B*, 103, 959-966 (2011).
8. L.S. Rothman et al., "The HITRAN2012 molecular spectroscopic database," *Journal of Quantitative Spectroscopy and Radiative Transfer*, 130, 4-50 (2013).
9. F. Thibault, R.Z. Martinez, J.L. Domenech, D. Bermejo, and J.-P. Bouanich, "Raman and infrared linewidths of CO in Ar," *Journal of Chemical Physics*, 117, 2523-2531 (2002).
10. A.W. Mantz, V.M. Devi, D.C. Benner, M.A.H. Smith, A. Predoi-Cross, and M. Dulick, "A multispectrum analysis of widths and shifts in the 2010-2260 cm−1 region of 12C16O broadened by Helium at temperatures between 80 and 297 K," *Journal of Molecular Structure*, 742, 99-110 (2005).
11. ASTM D6890, "Standard test method for determination of ignition delay and derived cetane number (DCN) of diesel fuel oils by combustion in a constant volume chamber," ASTM International (2013).
12. G.E. Bogin, A. DeFilippo, J.Y. Chen, G. Chin, J. Luecke, M.A. Ratcliff, B.T. Zigler, and A.M. Dean, "Numerical and experimental investigation of n-heptane autoignition in the ignition quality tester (IQT)," *Energy and Fuels*, 25 5562-5572 (2011).
13. S.M. Sarathy, C. Yeung, C.K. Westbrook, W.J. Pitz, M. Mehl, and M.J. Thomson, "An experimental and kinetic modeling study of n-octane and 2-methylheptane in an opposed-flow diffusion flame," *Combustion and Flame*, 158, 1277-1287 (2011).
14. Z. Luo, S. Som, S.M. Sarathy, M. Plmer, W.J. Pitz, D.E. Longman, and T. Lu, "Development and validation of an n-dodecane skeletal mechanism for spray combustion applications," *Combustion Theory and Modeling*, 18, 187-203 (2014).
15. L. Cai, H. Pitsch, S.Y. Mohamed, V. Raman, J. Bugler, H.J. Curran, and S.M. Sarathy, "Optimized reaction mechanism rate rules for ignition of normal alkanes," *Combustion and Flame*, 173, 468-482 (2016).
16. K. Narayanaswamy, P. Pepiot, and H. Pitsch, "A chemical mechanism for low to high temperature oxidation of n-dodecane as a component of transportation fuel surrogates," *Combustion and Flame*, 161, 866–884 (2014).
17. H. Wang, Y. Ra, M. Jia, and R.D. Reitz, "Development of a reduced n-dodecane-PAH mechanism and its application for n-dodecane soot predictions," *Fuel*, 13625–13636 (2014).

18. M. Mehl, G. Vanhove, W.J. Pitz, and E. Ranzi, "Oxidation and combustion of the n-hexene isomers: A wide range kinetic modeling study," *Combustion and Flame*, 155, 756-772 (2008).
19. G.A. Weisser, "Modelling of combustion and nitric oxide formation for medium-speed DI diesel engines: a comparative evaluation of zero- and three-dimensional approaches" ETH Dissertation No. 14465, ETH Zurich (2001).
20. A. Vandersickel, M. Hartmann, K. Vogel, Y.M. Wright, M. Fikri, R. Starke, and K. Boulouchos, "The autoignition of practical fuels at HCCI conditions: High-pressure shock tube experiments and phenomenological modeling," *Fuel*, 93, 492-501 (2012).
21. J. Zheng, D.L. Miller, and N.P. Cernansky, "A Global Reaction Model for the HCCI Combustion Process," SAE technical paper 2004-01-2950 (2004).
22. M. Schreiber, S.A. Sakak, A. Lingens, and F.J. Griffiths, "A reduced thermokinetic model for the autoignition of fuels with variable octane ratings," *Proceedings of the Combustion Institute* 25, 933-940 (1994).
23. S.M. Sarathy, C.K. Westbrook, M. Mehl, W.J. Pitz, C. Togbe, P. Dagaut, H. Wang, M.A. Oehlschlaeger, U. Niemann, K. Seshadri, P.S. Veloo, C. Ji, F.N. Egolfopoulos, and T. Lu, "Comprehensive chemical kinetic modeling of the oxidation of 2-methylalkanes from C7 to C20," *Combustion and Flame*, 158, 2338-2357(2011).
24. E. Ranzi, A. Frassoldati, R. Grana, A. Cuoci, T. Faravelli, A.P. Kelley, and C.K. Law, "Hierarchical and comparative kinetic modeling of laminar flame speeds of hydrocarbon and oxygenated fuels," *Progress in Energy and Combustion Science*, 38, 468-501(2012).
25. H. Wang, E. Dames, B. Sirjean, D.A. Sheen, R. Tango, A. Violi, J.Y.W. Lai, F.N. Egolfopoulos, D.F. Davidson, R.K. Hanson, C.T. Bowman, C.K. Law, W. Tsang, N.P. Cernansky, D.L. Miller, and R.P. Lindstedt, "A high-temperature chemical kinetic model of n-alkane (up to n-dodecane), cyclohexane, and methyl-, ethyl-, n-propyl and n-butyl-cyclohexane oxidation at high temperatures, JetSurF version 2.0," September 19, 2010 (http://web.stanford.edu/group/haiwanglab/JetSurF/JetSurF2.0/index.html).
26. M. Chaos and F.L. Dryer, "Chemical-kinetic modeling of ignition delay: Considerations in interpreting shock tube data," *International Journal of Chemical Kinetics*, 42, 143-150 (2010).
27. H.J. Curran, P. Gaffuri, W.J. Pitz, and C.K. Westbrook, "A comprehensive modeling study of n-heptane oxidation," *Combustion and Flame*, 114, 149-177 (1998).
28. S. Tanaka, F. Ayala, J.C. Keck, and J.B. Heywood, "Two-stage ignition in HCCI combustion and HCCI control by fuels and additives," *Combustion and Flame*, 132, 219-239 (2003).
29. J. Yanowitz, M.A. Ratcliff, R.L. McCormick, J.D. Taylor, and M.J. Murphy, "Compendium of experimental cetane numbers," National Renewable Energy Laboratory Report NREL/TP-5400-61693 (2014).
30. D. Darcy, H. Nakamura, C.J. Tobin, M. Mehl, W.K. Metcalfe, W.J. Pitz, C.K. Westbrook, and H.J. Curran, "An experimental and modeling study of surrogate mixtures of n-propyl- and n-butylbenzene in n-heptane to simulate n-decylbenzene ignition," *Combustion and Flame*, 161, 1460-1473 (2014).
31. H. Nakamura, D. Darcy, M. Mehl, C.J. Tobin, W.K. Metcalfe, W.J. Pitz, C.K. Westbrook, and H.J. Curran, "An experimental and modeling study of shock tube and rapid compression machine ignition of n-butylbenzene/air mixtures," *Combustion and Flame*, 161, 49-64 (2014).
32. D. Darcy, H. Nakamura, C.J. Tobin, M. Mehl, W.K. Metcalfe, W.J. Pitz, C.K. Westbrook, and H.J. Curran, "A high-pressure rapid compression machine study of n-propylbenzene ignition," *Combustion and Flame*, 161, 65-74 (2014).
33. E.R. Ritter and J.W. Bozzelli, "THERM: Thermodynamic property estimation for gas phase radicals and molecules" *International Journal of Chemical Kinetics*, 23, 767-778 (1991).

34. S.J. Blanksby and G.B. Ellison, “Bond dissociation energies of organic molecules” *Accounts of Chemical Research*, 36, 255-263 (2003).
35. P. Ghosh and S.B. Jaffe, “Detailed composition-based model for predicting the cetane number of diesel fuels,” *Industrial and Engineering Chemistry Research*, 45, 346-351 (2006).
36. V. Knop, M. Loos, C. Pera, and N. Jeuland, “A linear-by-mole blending rule for octane numbers of n-heptane/iso-octane/toluene mixtures,” *Fuel* 115, 666-673 (2014).
37. F.M. Haas and F.L. Dryer, “Application of blending rules for ignition quality metrics: A comment on 'A linear-by-mole blending rule for octane numbers of n-heptane/iso-octane/toluene mixtures’,” *Fuel* 120, 240-242 (2014).
38. F. Battin-Leclerc, “Detailed chemical kinetic models for the low-temperature combustion of hydrocarbons with application to gasoline and diesel fuel surrogates,” *Progress in Energy and Combustion Science*, 34, 440-498 (2008).

AFOSR Deliverables Submission Survey

Response ID:7309 Data

1.

Report Type

Final Report

Primary Contact Email

Contact email if there is a problem with the report.

oehlsm@rpi.edu

Primary Contact Phone Number

Contact phone number if there is a problem with the report

5182766626

Organization / Institution name

Rensselaer Polytechnic Institute

Grant/Contract Title

The full title of the funded effort.

(PECASE '10) The Oxidation and Autoignition of Jet Fuels

Grant/Contract Number

AFOSR assigned control number. It must begin with "FA9550" or "F49620" or "FA2386".

FA9550-11-1-0261

Principal Investigator Name

The full name of the principal investigator on the grant or contract.

Matthew Oehlschlaeger

Program Officer

The AFOSR Program Officer currently assigned to the award

Chiping Le

Reporting Period Start Date

09/15/2011

Reporting Period End Date

09/14/2016

Abstract

A series of experimental studies designed to elucidate the oxidative reactivity and ignition properties of jet fuel and its components under homogeneous (shock tube) and multiphase spray conditions are reported. The influences of molecular composition, fuel blending, fuel/air mixture, and thermodynamic condition on oxidation and ignition are quantified and targets for kinetic model and reacting flow simulation development are provided. The most important contribution of the project is the quantification of the differences in kinetic behavior and identification of reactivity timescales across the three kinetic temperature regimes of importance in combustion processes, the low, high, and NTC temperature regions.

Distribution Statement

This is block 12 on the SF298 form.

Distribution A - Approved for Public Release

Explanation for Distribution Statement

If this is not approved for public release, please provide a short explanation. E.g., contains proprietary information.

SF298 Form

Please attach your SF298 form. A blank SF298 can be found here. Please do not password protect or secure the PDF The maximum file size for an SF298 is 50MB.

SF+298+Oehlschlaeger+2.pdf

Upload the Report Document. File must be a PDF. Please do not password protect or secure the PDF . The maximum file size for the Report Document is 50MB.

Oehlschlaeger+final+report+2016.pdf

Upload a Report Document, if any. The maximum file size for the Report Document is 50MB.

Archival Publications (published) during reporting period:

A. Tekawade, G. Kosiba, M.A. Oehlschlaeger, "Time-Resolved Carbon Monoxide Measurements During the Low- to Intermediate-Temperature Oxidation of n-Heptane, n-Decane, and n-Dodecane," Combustion and Flame, 173, 402-410 (2016).

A. Tekawade, M.A. Oehlschlaeger, "An Experimental Study on the Spray Ignition of Alkanes," Fuel, 185, 381-393 (2016).

M. Huang, S. Gowdagiri, X.M. Cesari, M.A. Oehlschlaeger, "Diesel Engine CFD Simulations: Influence of Fuel Variability on Ignition Delay," Fuel, 181, 170-177 (2016).

S.M. Sarathy, G. Kukkadapu, T. Javed, A. Ahmed, A. Tekawade, M. Mehl, G. Kosiba, S. Park, M. El Rachidi, W.L. Roberts, M.A. Oehlschlaeger, C.J. Sung, A. Farooq, "Compositional Effects on the Ignition of FACE Gasolines," Combustion and Flame, 169, 171-193 (2016).

C.W. Zhou, Y. Li, E. O'Connor, K.P. Somers, S. Thion, C. Keesee, O. Mathieu, E.L. Petersen, T.A. DeVerter, M.A. Oehlschlaeger, G. Kukkadapu, C.J. Sung, M. Alrefae, F. Khaled, A. Farooq, P. Dirrenberger, P.A. Glaude, F. Battin-Leclerc, J. Santer, Y. Ju, T. Held, F.M. Haas, F.L. Dryer, H.J. Curran, "A Comprehensive Experimental and Modeling Study of Isobutene Oxidation," Combustion and Flame, 167, 353-379 (2016).

S.H. Won, F.M. Haas, A. Tekawade, G. Kosiba, M.A. Oehlschlaeger, S. Dooley, F.L. Dryer, "Combustion Characteristics of C4 iso-Alkane Oligomers: Experimental Characterization of iso-Dodecane as a Jet Fuel Surrogate Component," Combustion and Flame, 165, 137-143 (2016).

S.M. Burke, U. Burke, R. McDonagh, O. Mathieu, E.L. Petersen, W. Wang, M.A. Oehlschlaeger, B. Rhodes, R.K. Hanson, D. Davidson, B.W. Weber, C.J. Sung, J. Santer, Y. Ju, E.N. Volkov, A.A. Konnov, M. Alrefae, F. Khaled, A. Farooq, H.J. Curran, "An Experimental and Modeling Study of Propene Oxidation. Part 2: Ignition Delay Times and Flame Speeds," Combustion and Flame, 162, 296-314 (2015).

S.M. Sarathy, G. Kukkadapu, M. Mehl, W. Wang, T. Javed, S. Park, M.A. Oehlschlaeger, A. Farooq, W.J. Pitz, C.J. Sung, "Ignition of Alkane-Rich FACE Gasoline Fuels and their Surrogates," Proceedings of the Combustion Institute, 35, 249-257 (2015).

S. Gowdagiri, X.M. Cesari, M. Huang, M.A. Oehlschlaeger, "A Diesel Engine Study of Conventional and Alternative Diesel and Jet Fuels: Ignition and Emissions Characteristics," Fuel, 136, 253-260 (2014).

S. Gowdagiri, M.A. Oehlschlaeger, "A Global Reduced Model for Conventional and Alternative Jet and Diesel Fuel Autoignition," Energy and Fuels, 28, 2795-2801 (2014).

S. Gowdagiri, W. Wang, M.A. Oehlschlaeger, "A Shock Tube Ignition Delay Study of Conventional Diesel Fuel and Hydroprocessed Renewable Diesel Fuel from Algal Oil," Fuel, 128, 21-29 (2014).

S.M. Sarathy, T. Javed, F. Karsenty, A. Heufer, W. Wang, S. Park, A. Elwardany, A. Farooq, C.K. Westbrook, W.J. Pitz, M.A. Oehlschlaeger, G. Dayma, H.J. Curran, P. Dagaut, "Comprehensive Experimental and

Kinetic Modeling Study of 2,5-Dimethylhexane, an Iso-Paraffinic Surrogate for Transportation Fuels," Combustion and Flame, 161, 1444-1459 (2014).

S.H. Won, S. Dooley, P.S. Veloo, H. Wang, M.A. Oehlschlaeger, F.L. Dryer, Y. Ju, "The Combustion Properties of the Synthetic Diesel Fuel 2,6,10-Trimethyldodecane and a Molecular Analysis," Combustion and Flame, 161, 826-834 (2014).

H. Wang, W.J. Gerken, W. Wang, M.A. Oehlschlaeger, "Experimental Study of the High-Temperature Autoignition of Tetralin," Energy and Fuels, 27, 5483-5487 (2013).

P. Dievart, H.H. Kim, S.H. Won, Y. Ju, S. Dooley, F.L. Dryer, W. Wang, M.A. Oehlschlaeger, "The Combustion Properties of 1,3,5-Trimethylbenzene and a Kinetic Model," Fuel, 109, 125-136 (2013).

W. Wang, Z. Li, M.A. Oehlschlaeger, D. Healy, H.J. Curran, S.M. Sarathy, M. Mehl, W.J. Pitz, C.K. Westbrook, "An Experimental and Modeling Study of the Autoignition of 3-Methylheptane," Proceedings of the Combustion Institute, 34, 335-343 (2013).

S. Dooley, S.H. Won, S. Jahangirian, Y. Ju, F.L. Dryer, H. Wang, M.A. Oehlschlaeger, "The Combustion Kinetics of a Synthetic Paraffinic Jet Aviation Fuel and a Fundamentally Formulated, Experimentally Validated Surrogate Fuel," Combustion and Flame, 159, 3014-3020 (2012).

H. Wang, M.A. Oehlschlaeger, "Autoignition Studies of Conventional and Fischer-Tropsch Jet Fuels," Fuel, 98, 249-258 (2012).

New discoveries, inventions, or patent disclosures:

Do you have any discoveries, inventions, or patent disclosures to report for this period?

No

Please describe and include any notable dates

Do you plan to pursue a claim for personal or organizational intellectual property?

Changes in research objectives (if any):

Change in AFOSR Program Officer, if any:

Extensions granted or milestones slipped, if any:

AFOSR LRIR Number

LRIR Title

Reporting Period

Laboratory Task Manager

Program Officer

Research Objectives

Technical Summary

Funding Summary by Cost Category (by FY, $K)

	Starting FY	FY+1	FY+2
Salary			
Equipment/Facilities			
Supplies			
Total			

Report Document

Report Document - Text Analysis

Report Document - Text Analysis

Appendix Documents

2. Thank You

E-mail user

Dec 02, 2016 13:42:15 Success: Email Sent to: oehlsm@rpi.edu